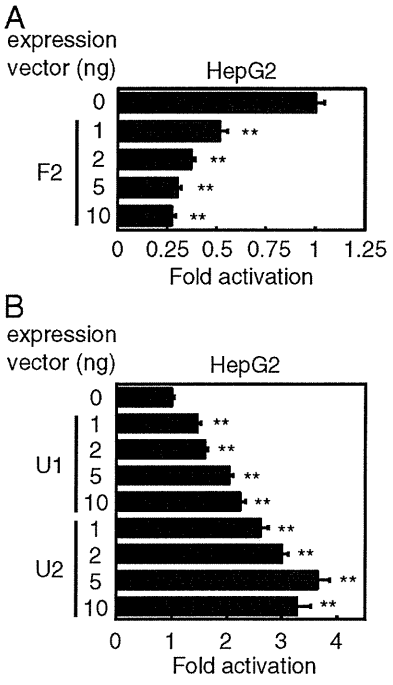

FIG. 4. Effect of overexpression of FOXA2 or USF on *hDIO1* promoter activity. −187/−4 hDIO1-Luc was transiently transfected into HepG2 cells in the presence of increasing amounts of vectors expressing FOXA2 (F2) (A) or USF1 or USF2 (U1 and U2, respectively) (B). Promoter activity was normalized to *Renilla* luciferase activity, then expressed as the relative activity to −187/−4 hDIO1-Luc cotransfected with pF4A without a cDNA insert. Statistical significance was determined by ANOVA followed by Dunnett's test. **, $P < 0.01$.

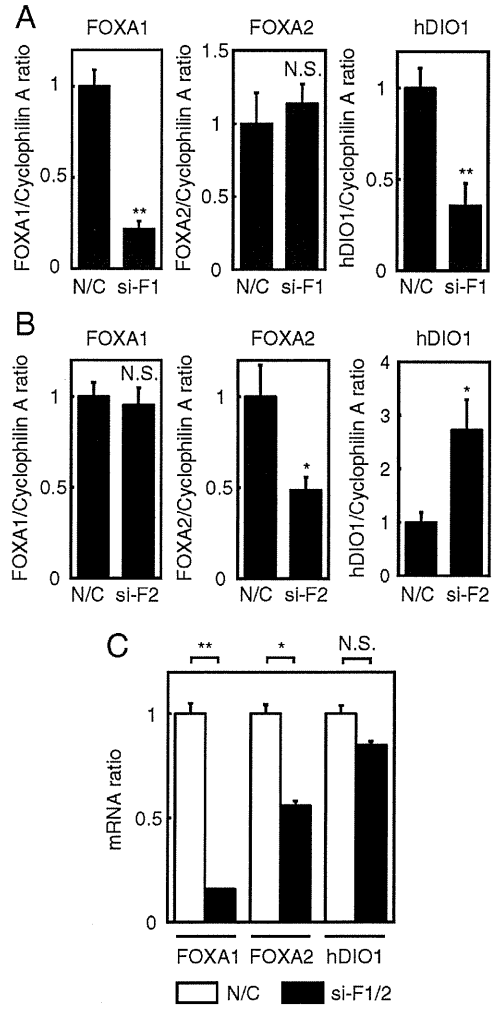

FIG. 5. Knockdown of FOXA1 and/or FOXA2. Effect of transfection of FOXA1 (A) and FOXA2 (B) siRNA on the mRNA expression level of FOXA1, FOXA2, and D1. Simultaneous knockdown of FOXA1 and FOXA2 (C) was performed using siRNA that has identical sequences in both FOXA1 and FOXA2. N/C, Negative control siRNA; si-F1, siRNA specific for FOXA1; si-F2, siRNA specific for FOXA2; si-F1/2, siRNA specific for both FOXA1 and FOXA2. mRNA expression level was normalized to that of cyclophilin A in each sample and expressed as the relative activity to the basal expression (N/C). Statistical significance was determined by unpaired *t* test. *, $P < 0.05$; **, $P < 0.01$. N.S., Not significant.

down of FOXA1 decreased the expression of *hDIO1* mRNA, and knockdown of FOXA2 increased the expression level of *hDIO1* mRNA. FOXA1 and FOXA2 did not affect each other's expression by knockdown of them (Fig. 5, A and B). In addition, when both FOXA1 and FOXA2 were knocked down simultaneously, no change in the expression of *hDIO1* mRNA was seen (Fig. 5C). Thus, *hDIO1* expression is positively regulated by FOXA1 and negatively regulated by FOXA2, and FOXA1 and FOXA2 interact with each other to regulate *hDIO1* expression.

Interaction between FOXA and USF in the activation of the *hDIO1* promoter

Transcription factors frequently interact to coordinately regulate gene expression, and we first wished to determine whether the FOXA binding site and the E-box present in the *hDIO1* promoter interact. We cotransfected a WT or mutated −187/−4 hDIO1-Luc construct and USF expression plasmids into HepG2 cells. When the FOXA binding site was mutated, the transcription activity of the *hDIO1* promoter in the presence of transfected USF was attenuated (Fig. 6A). Thus, activation of the *hDIO1* promoter by USF depends on the presence of a functional FOXA binding site. Next, we investigated the effects of FOXA on the response of the *hDIO1* promoter to USF. We knocked down the expression of FOXA and cotransfected a −187/−4 hDIO1-Luc construct along with USF expression plasmids into HepG2 cells. As shown in Fig. 6B, the transcription activity of the *hDIO1* promoter was attenuated by knockdown of FOXA1 and enhanced by knockdown of FOXA2. The transcription activity of the *hDIO1* promoter was also attenuated by simultaneous knockdown of FOXA1 and FOXA2 to an extent similar to that seen for the knockdown of FOXA1. The suppressed activity by knockdown of FOXA1 was not restored by overexpression of USF, and the enhanced activity by knockdown of FOXA2 was further enhanced by overexpression of USF. Thus, the response of the *hDIO1* pro-

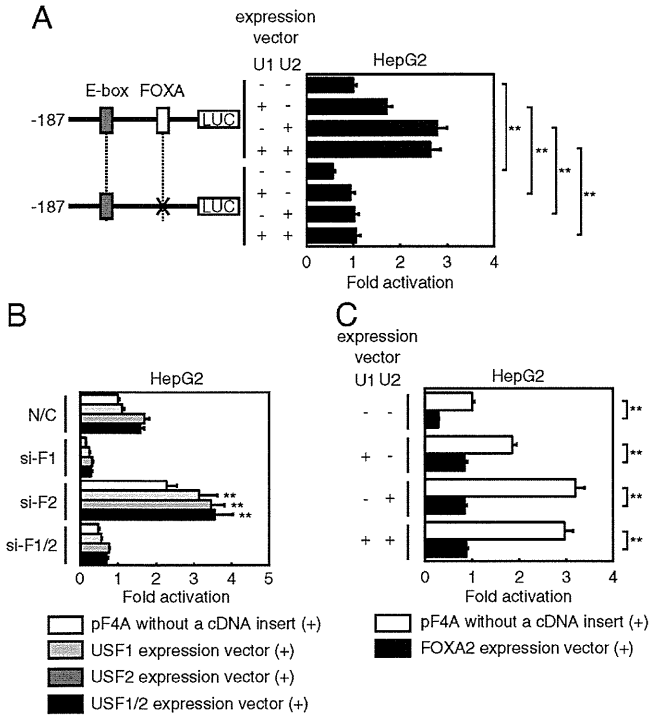

FIG. 6. Interaction between FOXA and USF in the activation of the *hDIO1* promoter. A, Dependence of the activation of *hDIO1* promoter by USF on the FOXA binding site. Schematic diagram in the *left* of figure representing WT and site-specific mutations of the *hDIO1* promoter, introduced into the upstream region of the luciferase gene. A *cross* represents the site-specific mutation of the putative FOXA binding site. Each construct was transiently cotransfected into HepG2 cells in the presence of 5 ng of vectors expressing USF1 (U1) and/or USF2 (U2). Promoter activity was normalized to *Renilla* luciferase activity, then expressed as the relative activity to −187/−4 hDIO1-Luc cotransfected with pF4A without a cDNA insert. Statistical significance was determined by ANOVA followed by Student-Newman-Keuls test. **, $P < 0.01$. B, Effect of knockdown of FOXA on the activation of the *hDIO1* promoter by USF. Short interfering RNA specific for FOXA1 and/or FOXA2 or a negative control siRNA were transfected into HepG2 cells as described in *Materials and Methods*. One day after siRNA transfection, −187/−4 hDIO1-Luc was transiently cotransfected in the presence of 5 ng of vectors expressing USF1 and/or USF2. N/C, Negative control siRNA; si-F1, siRNA specific for FOXA1; si-F2, siRNA specific for FOXA2; si-F1/2, siRNA specific for both FOXA1 and FOXA2. Promoter activity was normalized to *Renilla* luciferase activity, then expressed as the relative activity to −187/−4 hDIO1-Luc cotransfected with pF4A without a cDNA insert after knockdown by negative control siRNA. Statistical significance was determined by ANOVA followed by Student-Newman-Keuls test. **, $P < 0.01$ relative to −187/−4 hDIO1-Luc cotransfected with pF4A without a cDNA insert after knockdown by siRNA specific for FOXA2. C, Effect of overexpression of FOXA2 on the activation of the *hDIO1* promoter by USF. −187/−4 hDIO1-Luc was transiently transfected into HepG2 cells in the presence of 5 ng of vectors expressing USF1 (U1), USF2 (U2), and/or FOXA2. Promoter activity was normalized to *Renilla* luciferase activity, then expressed as the relative activity to −187/−4 hDIO1-Luc cotransfected with pF4A without a cDNA insert. Statistical significance was determined by ANOVA followed by Student-Newman-Keuls test. **, $P < 0.01$. LUC, Luciferase.

moter to USF was greatly attenuated by knockdown of FOXA1 and enhanced by knockdown of FOXA2. Furthermore, we cotransfected a −187/−4 hDIO1-Luc construct and USF expression plasmids with or without a FOXA2 expression plasmid into HepG2 cells. The transcription activity of the *hDIO1* promoter was enhanced in the presence of transfected USF (Fig. 6C, *white bar*), but the activity was greatly attenuated by cotransfection of the FOXA2 expression plasmid (Fig. 6C, *black bar*). Thus, the response of the *hDIO1* promoter to USF was attenuated by the coexpression of FOXA2. Collectively, these results indicate that FOXA1 is required for the activation of the *hDIO1* promoter by USF and that FOXA2 represses the transcription of *hDIO1* and disrupts the interaction of USF with FOXA1 by occupying the FOXA binding site.

Discussion

In this study, we analyzed the 5′-upstream region of *hDIO1* to identify protein-DNA interactions within the *hDIO1* promoter. Our experiments demonstrated that the region between nucleotides −187 and −132 is important for *hDIO1* promoter activity in HepG2 cells. We identified functional elements for FOXA and USF within this region, and we showed that these sites are important for the transcriptional regulation of *hDIO1*. Recently, Ohguchi *et al.* (9) identified a proximal hepatocyte nuclear factor (HNF)4α binding site in mice, and they demonstrated that the HNF4α binding site is essential for the activation of the mouse D1 gene by HNF4α. Deletion analyses of the 5′-flanking region of *hDIO1* were performed by Jakobs *et al.* (10) by transfecting 1.5- and 0.1-kb constructs into HepG2 cells, and they found that both constructs substantially increased luciferase activity compared with a promoterless vector. However, they did not perform a higher resolution promoter analysis, and we are the first to identify functional elements other than thyroid hormone responsive element in the *hDIO1* promoter.

The FOXA proteins were first identified as liver-enriched factors because of their ability to bind the transthyretin gene promoter, and they were originally termed HNF3 (11). There are three FOXA proteins, FOXA1 (HNF3α), FOXA2 (HNF3β), and FOXA3 (HNF3γ), which are encoded by different genes on different chromosomes (12). FOXA proteins play important roles in early embryonic development and organogenesis, and they are recognized as "pioneer factors" (13). In addition, the FOXA proteins control glucose metabolism through the regulation of multiple target genes in the liver, pancreas, and adipose tissue after birth (13). Our EMSA experiments demonstrated that FOXA1 and FOXA2 specifically bound the identical FOXA binding site of the *hDIO1* promoter. Although all three FOXA proteins exist relatively abundant in HepG2 cells (14) and recognize the same DNA sequences, slight differences in the binding affin-

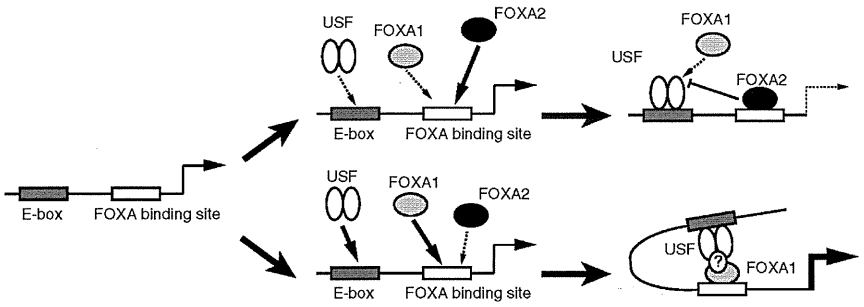

FIG. 7. A model for the regulation of liver-specific expression of *hDIO1* by FOXA1, FOXA2, and USF. FOXA1 and FOXA2 bind and share the identical FOXA binding site, and USF binds the E-box as a heterodimer. FOXA2 represses the transcription of *hDIO1* through the FOXA binding site (*upper panel*), and FOXA1 and USF work cooperatively to activate *hDIO1* transcription (*lower panel*).

ity and DNA binding capacity may account for their specificity (15). Indeed, there are very few reports that FOXA1 and FOXA2 share an identical binding site and coparticipate in the transcriptional regulation of a single gene (16). Our transfection assays and siRNA experiments demonstrated that *hDIO1* is positively regulated by FOXA1 and negatively regulated by FOXA2 and that FOXA1 and FOXA2 interact to coordinately regulate *hDIO1* expression. These results suggest that FOXA proteins are involved in thyroid hormone homeostasis.

USF proteins were first identified as regulators of adenovirus major late promoter transcription (17, 18). There are two USF proteins, 43 kDa (USF1) and 44 kDa (USF2), encoded by different genes on different chromosomes (19, 20). USF proteins primarily bind as dimers to consensus sequences containing the CACGTG motif termed an E-box (18, 19, 21). USF proteins are ubiquitously expressed, although different ratios of USF homo- and heterodimers are found in different cell types (22). The molecular details of USF binding and activity have been well characterized, but its biological role remains poorly understood. USF proteins regulate the expression of several genes related to glucose and lipid metabolism and peptide hormone synthesis, including liver-type pyruvate kinase (23) and glucokinase (24), fatty acid synthase (25), apolipoprotein A-II (26), calcitonin/calcitonin gene-related peptide (27), and ghrelin (8). In our study, we demonstrated that the putative E-box site in the *hDIO1* promoter specifically bound the USF1/USF2 heterodimer and that promoter activity increased in a dose-dependent manner with the cotransfection of the USF1/2 expression plasmid. These results suggest that USF positively regulate *hDIO1* expression. Additionally, promoter activity was almost completely abolished by mutation of the E-box motif, indicating that USF proteins are critical for the transcriptional regulation of *hDIO1* and thyroid hormone homeostasis in the liver and possibly kidney.

The response of the *hDIO1* promoter to USF was greatly attenuated by mutation of the FOXA binding site or knockdown of FOXA1, indicating that FOXA1 is necessary for the expression of *hDIO1* by USF. FOXA1 plays an essential role in the "pioneering" of gene regulatory elements, allowing for the recruitment of additional factors required for gene regulation (28), and our data suggest that USF cooperates with FOXA1 to regulate *hDIO1* promoter activity. Although we could not confirm the interaction between FOXA1 with USF by coimmunoprecipitation experiments in our experimental condition (data not shown), a direct physical interaction between FOXA1 and USF has been reported through the use of immunoprecipitation and glutathione *S*-transferase pull-down assays (29). Furthermore, the cooperation between FOXA1 and USF likely contributes to the liver-specific activation of *hDIO1*; although FOXA1 was expressed in both HepG2 and TSA201 cells in our preliminary experiments (data not shown), only HepG2 cells demonstrated substantial differences in promoter activity by transfection of −187/−4 hDIO1-Luc and mutation of the FOXA binding site. Interactions between cell-specific factors and other regulators are thought to contribute to the tissue-specific control of gene expression by the ubiquitous USF proteins (26, 30–34), and Fig. 7 shows our working model for the regulation of liver-specific expression of *hDIO1* by transcription factor binding to the −187 to −132 region of the *hDIO1* promoter. In this model, *hDIO1* promoter activity is modulated by FOXA1, FOXA2, and USF proteins, and these transcription factors interact with each other to fine-tune the *hDIO1* promoter activity.

In conclusion, we have shown that FOXA1, FOXA2, and USF regulate *hDIO1* expression in the liver. FOXA1 and FOXA2 both participate in the liver-specific regulation of *hDIO1* expression, and FOXA1 and USF act together to promote the liver-specific activation of *hDIO1*. FOXA1 and FOXA2 are likely involved in thyroid hormone homeostasis in the liver.

Acknowledgments

We thank Mami Yoshida and Yudai Takeuchi for technical assistance and Miyuki Ban for secretarial assistance.

Address all correspondence and requests for reprints to: Naotetsu Kanamoto, M.D., Ph.D., Department of Medicine and Clinical Science, Kyoto University Graduate School of Medicine, 54 Shogoin Kawahara-cho, Sakyo-ku, Kyoto 606-8507, Japan. E-mail: kyotetsu@kuhp.kyoto-u.ac.jp.

This work was supported by a Grant-in-Aid for Scientific Research from the Ministry of Health, the Labor and Welfare of Japan, Ministry of Education, Culture, Sports, Sciences, and Technology of Japan Grants 18790635, 19591075, and 21119013, and the Takeda Science Foundation.

Disclosure Summary: The authors have nothing to disclose.

References

1. Bianco AC, Salvatore D, Gereben B, Berry MJ, Larsen PR 2002 Biochemistry, cellular and molecular biology, and physiological roles of the iodothyronine selenodeiodinases. Endocr Rev 23:38–89
2. Berry MJ, Banu L, Larsen PR 1991 Type I iodothyronine deiodinase is a selenocysteine-containing enzyme. Nature 349:438–440
3. Toyoda N, Zavacki AM, Maia AL, Harney JW, Larsen PR 1995 A novel retinoid X receptor-independent thyroid hormone response element is present in the human type 1 deiodinase gene. Mol Cell Biol 15:5100–5112
4. Nagaya T, Fujieda M, Otsuka G, Yang JP, Okamoto T, Seo H 2000 A potential role of activated NF-κB in the pathogenesis of euthyroid sick syndrome. J Clin Invest 106:393–402
5. Moriyama K, Tagami T, Akamizu T, Usui T, Saijo M, Kanamoto N, Hataya Y, Shimatsu A, Kuzuya H, Nakao K 2002 Thyroid hormone action is disrupted by bisphenol A as an antagonist. J Clin Endocrinol Metab 87:5185–5190
6. Heinemeyer T, Wingender E, Reuter I, Hermjakob H, Kel AE, Kel OV, Ignatieva EV, Ananko EA, Podkolodnaya OA, Kolpakov FA, Podkolodny NL, Kolchanov NA 1998 Databases on transcriptional regulation: TRANSFAC, TRRD and COMPEL. Nucleic Acids Res 26:362–367
7. Piekielko-Witkowska A, Master A, Wojcicka A, Boguslawska J, Brozda I, Tanski Z, Nauman A 2009 Disturbed expression of type 1 iodothyronine deiodinase splice variants in human renal cancer. Thyroid 19:1105–1113
8. Kanamoto N, Akamizu T, Tagami T, Hataya Y, Moriyama K, Takaya K, Hosoda H, Kojima M, Kangawa K, Nakao K 2004 Genomic structure and characterization of the 5′-flanking region of the human ghrelin gene. Endocrinology 145:4144–4153
9. Ohguchi H, Tanaka T, Uchida A, Magoori K, Kudo H, Kim I, Daigo K, Sakakibara I, Okamura M, Harigae H, Sasaki T, Osborne TF, Gonzalez FJ, Hamakubo T, Kodama T, Sakai J 2008 Hepatocyte nuclear factor 4α contributes to thyroid hormone homeostasis by cooperatively regulating the type 1 iodothyronine deiodinase gene with GATA4 and Kruppel-like transcription factor 9. Mol Cell Biol 28:3917–3931
10. Jakobs TC, Schmutzler C, Meissner J, Köhrle J 1997 The promoter of the human type I 5′-deiodinase gene—mapping of the transcription start site and identification of a DR+4 thyroid-hormone-responsive element. Eur J Biochem 247:288–297
11. Lai E, Prezioso VR, Smith E, Litvin O, Costa RH, Darnell JE Jr 1990 HNF-3A, a hepatocyte-enriched transcription factor of novel structure is regulated transcriptionally. Genes Dev 4:1427–1436
12. Kaestner KH, Hiemisch H, Luckow B, Schütz G 1994 The HNF-3 gene family of transcription factors in mice: gene structure, cDNA sequence, and mRNA distribution. Genomics 20:377–385
13. Friedman JR, Kaestner KH 2006 The Foxa family of transcription factors in development and metabolism. Cell Mol Life Sci 63:2317–2328
14. Motallebipour M, Ameur A, Reddy Bysani MS, Patra K, Wallerman O, Mangion J, Barker MA, McKernan KJ, Komorowski J, Wadelius C 2009 Differential binding and co-binding pattern of FOXA1 and FOXA3 and their relation to H3K4me3 in HepG2 cells revealed by ChIP-seq. Genome Biol 10:R129
15. Yu X, Gupta A, Wang Y, Suzuki K, Mirosevich J, Orgebin-Crist MC, Matusik RJ 2005 Foxa1 and Foxa2 interact with the androgen receptor to regulate prostate and epididymal genes differentially. Ann NY Acad Sci 1061:77–93
16. Shimizu S, Miyamoto Y, Hayashi M 2002 Cell-type dependency of two Foxa/HNF3 sites in the regulation of vitronectin promoter activity. Biochim Biophys Acta 1574:337–344
17. Miyamoto NG, Moncollin V, Egly JM, Chambon P 1985 Specific interaction between a transcription factor and the upstream element of the adenovirus-2 major late promoter. EMBO J 4:3563–3570
18. Sawadogo M, Roeder RG 1985 Interaction of a gene-specific transcription factor with the adenovirus major late promoter upstream of the TATA box region. Cell 43:165–175
19. Gregor PD, Sawadogo M, Roeder RG 1990 The adenovirus major late transcription factor USF is a member of the helix-loop-helix group of regulatory proteins and binds to DNA as a dimer. Genes Dev 4:1730–1740
20. Sawadogo M, Van Dyke MW, Gregor PD, Roeder RG 1988 Multiple forms of the human gene-specific transcription factor USF. I. Complete purification and identification of USF from HeLa cell nuclei. J Biol Chem 263:11985–11993
21. Bendall AJ, Molloy PL 1994 Base preferences for DNA binding by the bHLH-Zip protein USF: effects of MgCl2 on specificity and comparison with binding of Myc family members. Nucleic Acids Res 22:2801–2810
22. Sirito M, Lin Q, Maity T, Sawadogo M 1994 Ubiquitous expression of the 43- and 44-kDa forms of transcription factor USF in mammalian cells. Nucleic Acids Res 22:427–433
23. Vallet VS, Casado M, Henrion AA, Bucchini D, Raymondjean M, Kahn A, Vaulont S 1998 Differential roles of upstream stimulatory factors 1 and 2 in the transcriptional response of liver genes to glucose. J Biol Chem 273:20175–20179
24. Iynedjian PB 1998 Identification of upstream stimulatory factor as transcriptional activator of the liver promoter of the glucokinase gene. Biochem J 333(Pt 3):705–712
25. Casado M, Vallet VS, Kahn A, Vaulont S 1999 Essential role in vivo of upstream stimulatory factors for a normal dietary response of the fatty acid synthase gene in the liver. J Biol Chem 274:2009–2013
26. Ribeiro A, Pastier D, Kardassis D, Chambaz J, Cardot P 1999 Cooperative binding of upstream stimulatory factor and hepatic nuclear factor 4 drives the transcription of the human apolipoprotein A-II gene. J Biol Chem 274:1216–1225
27. Lanigan TM, Russo AF 1997 Binding of upstream stimulatory factor and a cell-specific activator to the calcitonin/calcitonin gene-related peptide enhancer. J Biol Chem 272:18316–18324
28. Cirillo LA, McPherson CE, Bossard P, Stevens K, Cherian S, Shim EY, Clark KL, Burley SK, Zaret KS 1998 Binding of the winged-helix transcription factor HNF3 to a linker histone site on the nucleosome. EMBO J 17:244–254
29. Sun Q, Yu X, Degraff DJ, Matusik RJ 2009 Upstream stimulatory factor 2, a novel FoxA1-interacting protein, is involved in prostate-specific gene expression. Mol Endocrinol 23:2038–2047
30. Greenall A, Willingham N, Cheung E, Boam DS, Sharrocks AD 2001 DNA binding by the ETS-domain transcription factor PEA3 is regulated by intramolecular and intermolecular protein.protein interactions. J Biol Chem 276:16207–16215
31. Heckert LL 2001 Activation of the rat follicle-stimulating hormone receptor promoter by steroidogenic factor 1 is blocked by protein kinase a and requires upstream stimulatory factor binding to a proximal E box element. Mol Endocrinol 15:704–715
32. Ismail PM, Lu T, Sawadogo M 1999 Loss of USF transcriptional activity in breast cancer cell lines. Oncogene 18:5582–5591
33. Martin CC, Svitek CA, Oeser JK, Henderson E, Stein R, O'Brien RM 2003 Upstream stimulatory factor (USF) and neurogenic differentiation/β-cell E box transactivator 2 (NeuroD/BETA2) contribute to islet-specific glucose-6-phosphatase catalytic-subunit-related protein (IGRP) gene expression. Biochem J 371:675–686
34. Qyang Y, Luo X, Lu T, Ismail PM, Krylov D, Vinson C, Sawadogo M 1999 Cell-type-dependent activity of the ubiquitous transcription factor USF in cellular proliferation and transcriptional activation. Mol Cell Biol 19:1508–1517

point on the graph of the meta-regression where the lower 95% prediction band intersects with the horizontal (no-effect) axis. An STE using negatively controlled trials has been demonstrated for low-density lipoprotein cholesterol and statin therapy[12] and, more recently, for diastolic and systolic blood pressure and antihypertensive therapy (KJ and M Lassere, unpublished data).

In summary, in comparison with stroke prevention, there is a shortage of trials demonstrating that treatment-associated differences in achieved levels of albuminuria or estimated glomerular filtration rate translate into reductions in important outcomes. Without these, one cannot substantiate an argument for the use of albuminuria or estimated glomerular filtration rate as a surrogate in treatment decisions. Stevens *et al.*,[13] in a recent review, suggest that a by-trial analysis of studies measuring both proteinuria and renal outcomes is feasible with published data. Until such analyses are available, there will remain uncertainty surrounding treatment or policy recommendations based on these risk factors.

DISCLOSURE
The author declared no competing interests.

REFERENCES

1. van der Velde M, Matsushita K, Coresh J *et al.* Lower estimated glomerular filtration rate and higher albuminuria are associated with all-cause and cardiovascular mortality. A collaborative meta-analysis of high-risk population cohorts. *Kidney Int* 2011; **79**: 1341–1352.
2. Astor BC, Matsushita K, Gansevoort RT *et al.* Lower estimated glomerular filtration rate and higher albuminuria are associated with mortality and end-stage renal disease. A collaborative meta-analysis of kidney disease population cohorts. *Kidney Int* 2011; **79**: 1331–1340.
3. Thompson S, Pocock S. Can meta-analysis be trusted? *Lancet* 1991; **338**: 127–130.
4. Collins R, Peto R, MacMahon S *et al.* Blood pressure, stroke, and coronary heart disease. Part 2, short-term reductions in blood pressure: overview of randomised drug trials in their epidemiological context. *Lancet* 1990; **335**: 827–838.
5. Peto R. Why do we need systematic overviews of randomized trials? *Stat Med* 1987; **6**: 233–244.
6. Bailar J. The practice of meta-analysis. *J Clin Epidemiol* 1995; **48**: 149–157.
7. Thompson SD. Why sources of heterogeneity in meta-analysis should be investigated. *BMJ* 1994; **309**: 1351–1355.
8. Preliminary report: effect of encainide and flecainide on mortality in a randomized trial of arrhythmia suppression after myocardial infarction. The Cardiac Arrhythmia Suppression Trial (CAST) Investigators. *N Engl J Med* 1989; **321**: 406–412.
9. Packer M, Carver J, Rodeheffer R *et al.* Effect of oral milrinone on mortality in severe chronic heart failure. The PROMISE Study Research Group. *N Engl J Med* 1991; **325**: 1468–1475.
10. Lassere MN. The Biomarker-Surrogacy Evaluation Schema: a review of the biomarker-surrogate literature and a proposal for a criterion-based, quantitative, multidimensional hierarchical levels of evidence schema for evaluating the status of biomarkers as surrogate endpoints. *Stat Methods Med Res* 2008; **17**: 303–340.
11. Law MR, Morris JK, Wald NJ. Use of blood pressure lowering drugs in the prevention of cardiovascular disease: meta-analysis of 147 randomised trials in the context of expectations from prospective epidemiological studies. *BMJ* 2009; **338**: b1665.
12. Johnson KR, Freemantle N, Anthony DM *et al.* LDL-cholesterol differences predicted survival benefit in statin trials by the surrogate threshold effect (STE). *J Clin Epidemiol* 2009; **62**: 328–336.
13. Stevens L, Greene T, Levey A. Surrogate end points for clinical trials of kidney disease progression. *Clin J Am Soc Nephrol* 2006; **1**: 874–884.

see original article on page 1302

PPAR-α transcriptional activity is required to combat doxorubicin-induced podocyte injury in mice

Kiyoshi Mori[1], Masashi Mukoyama[1] and Kazuwa Nakao[1]

Immunosuppressants and inhibitors of the renin angiotensin system are major reagents to treat nephrotic syndrome, but their clinical effects are not necessarily satisfactory. Injection of doxorubicin in several strains of mice causes nephrotic syndrome–like disorder. Zhou *et al.* report that PPAR-α expression is downregulated in murine doxorubicin nephropathy and a PPAR-α agonist, fenofibrate, partially ameliorates the disorder induced likely through stabilization of nephrin expression and suppression of apoptosis in podocytes, providing a new preventive strategy.

Kidney International (2011) **79,** 1274–1276; doi:10.1038/ki.2011.36

Podocyte injury plays an important role in various proteinuric disorders. Because podocytes in adult humans and rodents have little proliferative activity, cellular stress in podocytes tends to accumulate, and podocyte loss cannot be recovered.[1] Therefore, protection of podocytes in renal disorders should be a major strategy to prevent worsening of renal failure, especially in chronic disease, but drugs clinically available for that goal are not very effective.

[1]*Department of Medicine and Clinical Science, Kyoto University Graduate School of Medicine, Sakyo-ku, Kyoto, Japan*
Correspondence: *Kiyoshi Mori, Department of Medicine and Clinical Science, Kyoto University Graduate School of Medicine, 54 Shogoin Kawahara-cho, Sakyo-ku, Kyoto 606-8507 Japan. E-mail: keyem@kuhp.kyoto-u.ac.jp*

Peroxisome proliferator-activated receptors (PPARs) possess various activities, including not only enhancement of fatty acid oxidization but also suppression of inflammation, apoptosis, and fibrosis.[2] Fenofibrate is a PPAR-α agonist widely used to treat hypertriglyceridemia patients, and its use may also be beneficial for cardiovascular disorders. Animal studies have shown that treatment with PPAR-α ligand or transgenic overexpression of PPAR-α in proximal tubules can ameliorate the development of cisplatin-induced or renal ischemia/reperfusion-induced acute kidney injury and diabetic nephropathy.[3,4]

Doxorubicin (adriamycin, or DOX) is an anthracycline class of chemotherapy reagent used to treat solid or hematopoietic

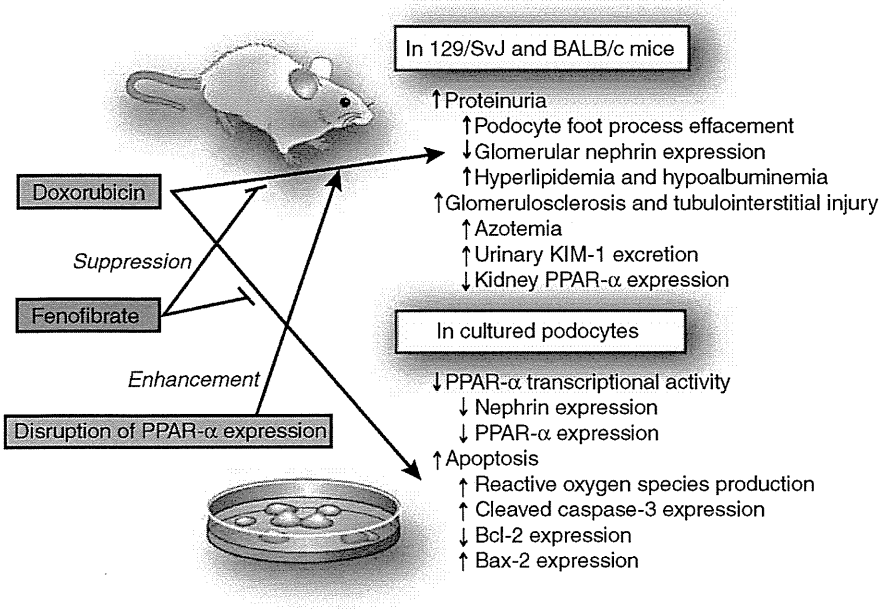

Figure 1 | Proposed mechanism of doxorubicin-induced nephropathy in disease-susceptible mouse strains. Treatment with fenofibrate attenuates the injury, whereas PPAR-α knockout mice show more severe renal phenotypes than wild-type mice do.[7] Not all combinations were examined by Zhou *et al.*[7]

malignancies. DOX causes glomerulosclerosis and tubulointerstitial injury in several selected strains of mice.[5] Docosahexaenoic acid (a PPAR agonist) ameliorates DOX-induced apoptosis of renal tubular cells.[6] Zhou *et al.*[7] (this issue) investigated whether fenofibrate inhibits podocyte injury and proteinuria in DOX-induced nephropathy among two murine strains. The BALB/c strain of mouse is highly susceptible to nephrotoxic effects of DOX, whereas C57BL/6 mice are resistant.[5] In PPAR-α knockout (KO) mice on a 129/SvJ background, which has usually been used in earlier studies to generate KO mice, intravenous challenge of DOX caused more severe renal damage among KO mice than among wild-type mice.[7] Renal disorder on a 129/SvJ background was slightly milder than, but basically similar to, that on a BALB/c background. Furthermore, fenofibrate partially suppressed the development of DOX nephropathy in both strains. PPAR-α KO mice grew up with almost normal kidneys, whereas DOX treatment reduced glomerular PPAR-α mRNA expression. These findings suggest that a certain level of PPAR-α activity is required to maintain normal glomerular structure under stressed conditions. Importantly, inhibition of DOX nephropathy by fenofibrate was not observed in PPAR-α KO mice; this excludes a possibility of off-target effects by fenofibrate. The *in vivo* and *in vitro* findings are summarized in Figure 1 (ref. 7).

Cardiotoxicity is a major side effect of DOX in humans, whereas proteinuria or acute renal failure is not so common. These observations suggest the presence of modifier genes that affect the sensitivity of organs and animals to DOX. Continual effort to identify genes that confer susceptibility in mice has recently led to the conclusion that mutation in protein kinase, DNA-activated, catalytic polypeptide (*Prkdc*) gene and subsequent depletion of mitochondrial DNA in the kidney after DOX treatment are the mechanism of DOX nephropathy in mice.[5] *Prkdc* plays an important role in DNA repair and maintenance of mitochondrial DNA integrity, especially in non-replicating cells such as podocytes and cardiocytes.

Diabetic nephropathy, which is usually accompanied by massive proteinuria, is almost pandemic, acting as the leading cause of end-stage renal failure. Antiproteinuric actions of fenofibrate have been reported in rodents and humans, but the evidence is, unfortunately, not very strong. Fenofibrate treatment of type 2 diabetic mice resulted in dramatic suppression of nephropathy, but the effects appear to be mediated largely by normalization of hyperglycemia.[8] After streptozotocin treatment to cause diabetes, PPAR-α KO mice exhibited more pronounced renal histological changes than wild-type mice at 4 months, but albuminuria in KOs was not greater than that in controls until 2 months.[9] Furthermore, PPAR-α protein expression was elevated threefold in diabetic mice compared with controls,[9] as opposed to reduced expression in DOX nephropathy.[7] In a large-scale human trial, treatment of type 2 diabetes patients with fenofibrate reduced albuminuria progression,[10] but renoprotective effects of fenofibrate have not been convincingly reproduced in following trials. Glomerular filtration rate may be suppressed by fenofibrate through inhibition of vasodilatory prostaglandin synthesis,[3] but an adequate correction of glomerular hyperfiltration might be renoprotective in the long term, as we have learned from blockade of the renin–angiotensin system.

A lot of future study has to be done to determine whether mitochondrial DNA damage in podocytes is a frequent cause, or simply a result, of proteinuric disorders, and whether its correction leads to preservation of renal function in human disorders. Furthermore, renoprotective effects of fenofibrate should be tested in large-scale, long-term human trials whose primary end points are progression of proteinuria and renal dysfunction.

DISCLOSURE
The authors declared no competing interests.

REFERENCES

1. Shankland SJ. The podocyte's response to injury: role in proteinuria and glomerulosclerosis. *Kidney Int* 2006; **69**: 2131–2147.
2. Michalik L, Wahli W. Involvement of PPAR nuclear receptors in tissue injury and wound repair. *J Clin Invest* 2006; **116**: 598–606.
3. Hiukka A, Maranghi M, Matikainen N *et al.* PPARalpha: an emerging therapeutic target in diabetic microvascular damage. *Nat Rev Endocrinol* 2010; **6**: 454–463.
4. Li S, Nagothu KK, Desai V *et al.* Transgenic expression of proximal tubule peroxisome proliferator-activated receptor-alpha in mice confers protection during acute kidney injury. *Kidney Int* 2009; **76**: 1049–1062.

5. Papeta N, Zheng Z, Schon EA *et al.* Prkdc participates in mitochondrial genome maintenance and prevents adriamycin-induced nephropathy in mice. *J Clin Invest* 2010; **120**: 4055–4064.
6. Lin H, Hou CC, Cheng CF *et al.* Peroxisomal proliferator-activated receptor-alpha protects renal tubular cells from doxorubicin-induced apoptosis. *Mol Pharmacol* 2007; **72**: 1238–1245.
7. Zhou Y, Kong X, Zhao P *et al.* Peroxisome proliferator-activated receptor-α is renoprotective in doxorubicin-induced glomerular injury. *Kidney Int* 2011; **79**: 1302–1311.
8. Park CW, Zhang Y, Zhang X *et al.* PPARalpha agonist fenofibrate improves diabetic nephropathy in db/db mice. *Kidney Int* 2006; **69**: 1511–1517.
9. Park CW, Kim HW, Ko SH *et al.* Accelerated diabetic nephropathy in mice lacking the peroxisome proliferator-activated receptor alpha. *Diabetes* 2006; **55**: 885–893.
10. Keech A, Simes RJ, Barter P *et al.* Effects of long-term fenofibrate therapy on cardiovascular events in 9795 people with type 2 diabetes mellitus (the FIELD study): randomised controlled trial. *Lancet* 2005; **366**: 1849–1861.

Significance of Adrenocorticotropin Stimulation Test in the Diagnosis of an Aldosterone-Producing Adenoma

Takuhiro Sonoyama, Masakatsu Sone, Kazutoshi Miyashita, Naohisa Tamura, Kenichi Yamahara, Kwijun Park, Naofumi Oyamada, Daisuke Taura, Megumi Inuzuka, Katsutoshi Kojima, Kyoko Honda, Yasutomo Fukunaga, Naotetsu Kanamoto, Masako Miura, Akihiro Yasoda, Hiroshi Arai, Hiroshi Itoh, and Kazuwa Nakao

Department of Medicine and Clinical Science, Kyoto University Graduate School of Medicine, Sakyo-ku, Kyoto 606-8507, Japan

Context: Adrenal venous sampling is the "gold standard" test in the diagnosis of an aldosterone-producing adenoma (APA) among patients with primary aldosteronism (PA) but is available only in specialized medical centers. Meanwhile, an APA is reported to be generally more sensitive to ACTH than idiopathic hyperaldosteronism.

Objective: The aim was to evaluate the diagnostic accuracy of the ACTH stimulation test in the diagnosis of an APA among those with suspicion of PA.

Patients and Setting: Fifty-nine patients admitted to Kyoto University Hospital on suspicion of PA were included in the study.

Interventions: ACTH stimulation tests with 1-mg dexamethasone suppression were performed.

Main Outcome Measure: Plasma aldosterone concentrations (PAC) were examined every 30 min after ACTH stimulation. Receiver-operated characteristics curve analysis was used to evaluate the diagnostic accuracy.

Results: PAC after ACTH stimulations were significantly higher in patients with an APA than in patients with idiopathic hyperaldosteronism or non-PA. Receiver-operated characteristics curve analyses showed that the PAC after ACTH stimulation was effective for the diagnosis of an APA among patients suspected of PA. The diagnostic accuracy was highest at 90 min after ACTH injection, with the optimal cutoff value greater than 37.9 ng/dl corresponding with sensitivity and specificity of 91.3 and 80.6% for the diagnosis of an APA.

Conclusions: Our study indicates that the ACTH stimulation test is useful in the diagnosis of an APA among patients suspected of PA. This test can be used to select patients who are highly suspected of an APA and definitely require adrenal venous sampling. ***(J Clin Endocrinol Metab* 96: 2771–2778, 2011)**

Primary aldosteronism (PA) is a major cause of secondary hypertension. The incidence of PA in hypertensive patients was thought to be less than 1%, but recent studies have shown that it is far more common than previously perceived (1–6). The diagnosis of PA should not be missed because it has been reported that patients with PA exhibit higher rates of cardiovascular and renal complications compared with those with essential hypertension

ISSN Print 0021-972X ISSN Online 1945-7197
Printed in U.S.A.

doi: 10.1210/jc.2011-0573 Received March 3, 2011. Accepted June 24, 2011.
First Published Online July 13, 2011

Abbreviations: A/C, Aldosterone to cortisol ratio; AII, angiotensin II; AII-R, AII-responsive; AII-U, AII-unresponsive; APA, aldosterone-producing adenoma; ARR, aldosterone renin ratio; AUC, area under the curve; AVS, adrenal venous sampling; CLR, contralateral ratio; CT, computed tomography; IHA, idiopathic hyperaldosteronism; LR, lateralization ratio; PA, primary aldosteronism; PAC, plasma aldosterone concentration; PRA, plasma renin activity; ROC, receiver-operated characteristic.

(7–10). The ratio of plasma aldosterone concentration (PAC) over plasma renin activity (PRA) [aldosterone renin ratio (ARR)] is usually used to screen for PA (11, 12). A positive ARR should always be confirmed by a follow-up test, such as captopril challenge test (11, 13), saline infusion test (11, 14), oral sodium-loading test (11, 15), and fludrocortisone suppression test (11, 16).

If a diagnosis of PA is made, the subtype should be identified. PA has two major subtypes; aldosterone-producing adenoma (APA) and idiopathic hyperaldosteronism (IHA) (17). In patients with an APA, hypersecretion of aldosterone is usually from one adrenal gland, whereas in those with IHA, hypersecretion of aldosterone is from both adrenal glands. Although rarer forms of PA exist, APA and IHA account for more than 95% of all PA cases. The differential diagnosis of these subtypes is crucial because an APA can be cured surgically, whereas bilateral IHA should be treated medically.

Imaging tests, such as computed tomography (CT) are initially used to classify the subtype and exclude a carcinoma (11). However, CT findings are often misleading (18, 19). One reason is that APA are frequently less than 1 cm in diameter, a size that is sometimes difficult to detect by CT scanning. Another reason is that a mass found on CT is sometimes nonfunctioning.

Adrenal venous sampling (AVS) is the current "gold standard" test to distinguish between unilateral and bilateral PA (11, 19). The procedure is recommended before surgery for patients with PA to avoid the risk of unilateral adrenalectomy of the wrong side (11, 12). However, it is not widely available because AVS requires an experienced angiographer who can locate the small right adrenal vein and take blood samples from adrenal veins (20). Also, AVS is an invasive procedure, somewhat risky, and costly (20). Therefore, AVS is largely limited to specialized major tertiary centers. Adrenal scintigraphy with ^{131}I-6β-iodomethyl-19-norcholesterol under dexamethasone suppression is another method used in the differential diagnosis of an APA or IHA (21). However, the sensitivity of this test largely depends on the size of the tumor because tracer uptake is poor in an APA less than 1 cm in diameter (21, 22). Like AVS, this test is not widely available. Therefore, it would be better if there was an easy method to select patients who are highly suspicious of an APA and definitely need AVS.

In prior years, the posture stimulation test was used to distinguish between an APA and IHA (23, 24). This test was based on the observation that the PAC in IHA patients increased when they changed from a supine to a standing position, owing to enhanced sensitivity of the adrenal zona glomerulosa to changes in angiotensin II (AII) (25, 26). Conversely, APA were considered to be unresponsive to AII stimulation. Later reports, however, showed that AII-responsive (AII-R) APA account for a considerable portion of APA (27–29). AII-R APA are difficult to distinguish from IHA by posture stimulation test because, in the cases of AII-R APA, the PAC responds as well to upright posture as IHA (27). In fact, data show that the posture stimulation test had a relatively low diagnostic accuracy in the differential diagnosis between an APA and IHA (30, 31). Meanwhile, PAC of both AII-unresponsive (AII-U) APA and AII-R APA cases were reported to be more responsive to ACTH stimulation than those of IHA cases (28), although there are reports of ACTH-responsive IHA cases (32).

The present study was performed to test the hypothesis that this difference in sensitivity to ACTH could be useful in the diagnosis of an APA among patients suspected of PA. To address this hypothesis, we tested the efficiency of the ACTH stimulation test under 1-mg dexamethasone suppression.

Patients and Methods

We retrospectively analyzed the medical records of patients with suspected PA who were admitted to the Department of Endocrinology and Metabolism of Kyoto University Hospital, Kyoto, Japan, over the past 7 yr. The study was approved by the Kyoto University Graduate School and Faculty of Medicine Ethics Committee and conducted in accordance with the principles of the Declaration of Helsinki. Patients with an ARR over 20 ng/dl per ng/ml · h who were admitted to our hospital were initially included (12). All antihypertensive drugs except calcium channel blockers and α-blockers were stopped at least 2 wk before hospitalization. Patients with hypokalemia (*i.e.* serum potassium levels <3.5 mEq/liter) were allowed to take oral potassium supplementation.

Blood pressures were measured in a quiet and warm room with patients in the seated position with the arm held at heart level. The blood pressures described in Table 1 were those obtained the morning after hospitalization. All tests were performed during morning hours in a quiet room. PRA and PAC were measured in blood samples obtained after 30 min of rest in a supine position in the morning. We used the captopril challenge test to confirm diagnosis of PA in this study. An ARR of at least 20 ng/dl per ng/ml · h at 60 min after administration of 50 mg of captopril was considered positive for PA; a post-captopril ARR below 20 ng/dl per ng/ml · h indicated non-PA (12).

Patients with confirmed PA underwent subtype diagnosis before surgery. Adrenal CT scanning was done for initial localization. The definitive tests for subtype diagnosis were AVS. AVS was performed by expert radiologists with ACTH stimulation as we previously described (33). Adrenal vein cannulation was considered successful if the adrenal vein/inferior vena cava cortisol gradient (selectivity index) was greater than 3.0. We considered lateralization when the aldosterone to cortisol ratio (A/C) from one adrenal gland was at least three times the ratio from the other adrenal gland [lateralization ratio (LR)] and the A/C in the contralateral adrenal vein was lower than the A/C in the vena cava [contralateral ratio (CLR)] (19). When the CLR was greater than 1.0 and the LR was no greater than 3.0 in a patient with con-

TABLE 1. Baseline characteristics of the patients of each group

	IHA group	*P* value IHA *vs.* APA	APA group	*P* value APA *vs.* non-PA	Non-PA group[a]
n	16		23		20
Age (yr)	57.8 ± 3.0	ns	48.4 ± 3.1	ns	51.7 ± 2.2
Sex (males:females)	7:9		12:11		13:7
Basal PAC (pg/ml)	166.1 ± 21.1	$P < 0.05$	368.2 ± 60.9	$P < 0.005$	150.2 ± 12.4
Basal PRA (ng/ml · h)	0.39 ± 0.10	ns	0.31 ± 0.07	$P < 0.001$	0.95 ± 0.18
U-Aldo (μg/d)	10.2 ± 1.1	$P < 0.01$	19.7 ± 2.6	$P < 0.01$	11.6 ± 1.0
Serum K (mEq/liter)	3.67 ± 0.09	ns	3.39 ± 0.11	$P < 0.001$	3.83 ± 0.07
Systolic BP (mm Hg)[b]	127.5 ± 4.9	ns	135.7 ± 3.7	$P < 0.05$	125.7 ± 3.5
Diastolic BP (mm Hg)[a]	78.1 ± 3.0	ns	87.7 ± 2.6	ns	83.2 ± 2.9

Data are expressed as means ± SEM. U-Aldo, Urinary aldosterone; K, potassium; BP, blood pressure; ns, not significant.

[a] Non-PA group in this study indicates a group of patients who were positive for the screening test of PA (*i.e.* an ARR ≥20 ng/dl per ng/ml · h) but were negative for captopril challenge test.

[b] 80% of the non-PA group, 87.5% of the IHA group, and 87.0% of the APA group were taking antihypertensive agents.

firmed PA, bilateral aldosterone secretion was considered. As shown in *Exclusion criteria* below, those with an ambiguous AVS outcome (*i.e.* LR >3.0 and CLR >1.0, or LR ≤3.0 and CLR ≤1.0) were excluded from this study.

Diagnosis of an APA required the following: 1) diagnosis of PA by the captopril challenge test; 2) lateralization of aldosterone secretion at AVS; and 3) CT evidence of adrenal mass and/or pathological evidence of adrenal adenoma in the adrenal gland with aldosterone hypersecretion. Patients with confirmed PA for whom bilateral aldosterone hypersecretion was confirmed by AVS were diagnosed with IHA.

Exclusion criteria

The following patients were excluded from this study: confirmed PA with no acceptable subtype diagnosis; unsuccessful AVS; ambiguous AVS outcomes (*i.e.* LR >3.0 and CLR >1.0, or LR ≤3.0 and CLR ≤1); a negative post-captopril ARR with a pathologically confirmed APA; and autonomous cortisol secretion (*i.e.* plasma cortisol level ≥3.0 μg/dl after overnight 1-mg dexamethasone suppression).

ACTH stimulation test under 1-mg dexamethasone suppression

ACTH stimulation tests under 1-mg dexamethasone suppression were performed on all patients. Dexamethasone was administered at 2300 h the night before ACTH injection to avoid the effect of endogenous ACTH. At 0800 h the following morning, 0.25 mg (25 IU) of synthetic ACTH (cosyntropin) was injected, and blood samples were taken every 30 min until 120 min after the injection. We examined the PAC values before and after ACTH injection (PAC_{0min}, PAC_{30min}, PAC_{60min}, PAC_{90min}, and PAC_{120min}) and the fold increase from PAC_{0min} after ACTH injection (PAC_{30min}/PAC_{0min}, PAC_{60min}/PAC_{0min}, PAC_{90min}/PAC_{0min}, and PAC_{120min}/PAC_{0min}).

Statistical analysis

All the data are expressed as mean ± SEM. We used one-way ANOVA followed by *post hoc* Tukey's multiple comparison test to compare means between groups. A P value <0.05 was considered to be statistically significant. The diagnostic accuracy of different time points used to analyze outcomes of the ACTH stimulation test was assessed with a receiver-operated characteristics (ROC) curve and the area under the ROC curve (AUC). When the variable under study could not be distinguished between groups, the AUC was 0.5 (*e.g.* the ROC curve coincided with the diagonal). When there were no overlapping values between the groups, the AUC equaled 1 and the ROC curve reached the upper left corner of the plot. The optimal cutoff point of each time point (*i.e.* the best combination of sensitivity and the lowest false-positive rate) was set at the closest point to the upper left corner of the ROC curve plot.

Results

We analyzed 80 consecutive patients with a positive screening test of an ARR greater than 20 ng/dl per ng/ml · h who were admitted to our hospital for the diagnosis of PA. Of these patients, 20 were diagnosed with non-PA (the non-PA group; *i.e.* screening-positive and confirmation-negative group) by captopril challenge test. The following patients were excluded from the study: three patients with confirmed PA who did not undergo AVS; seven patients with unsuccessful AVS; four with ambiguous AVS results; four with a negative post-captopril ARR with a pathologically confirmed APA; and three patients with autonomous cortisol secretion. The remaining patients were classified as belonging to either the IHA or APA group, according to criteria defined in *Patients and Methods*.

A total of 59 patients were included in this study: 20 in the non-PA group (*i.e.* screening-positive and confirmation-negative group), 16 in the IHA group, and 23 in APA group (Fig. 1). All but three APA patients underwent laparoscopic adrenalectomy, and all those who underwent surgery had pathologically confirmed adrenal adenoma.

Baseline characteristics

Baseline characteristics of the IHA, APA, and non-PA groups are shown in Table 1. Patients with IHA and

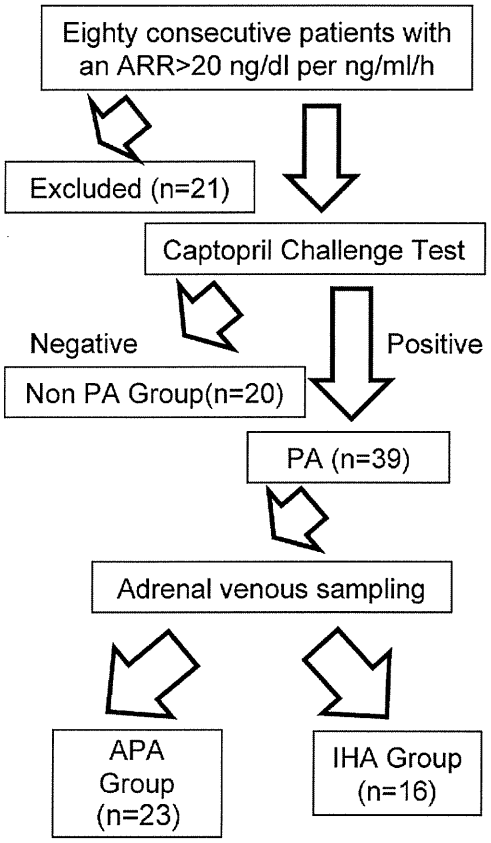

FIG. 1. Trial design.

APA had significantly lower basal PRA levels than those of non-PA ($P < 0.05$ and $P < 0.001$, respectively). Basal PRA levels did not differ significantly between patients in the IHA and APA groups. Basal PAC levels were significantly higher in the APA group compared with the IHA and non-PA groups ($P < 0.005$ and $P < 0.001$, respectively). The APA group also had significantly higher urinary aldosterone levels than the IHA and non-PA groups ($P < 0.01$ and $P < 0.01$, respectively). Serum K levels were significantly lower in the APA *vs.* the non-PA group ($P < 0.001$); 87.5% of the IHA group, 87.0% of the APA, and 80% of the non-PA group were taking antihypertensive agents. In the IHA group, 31.3% of patients were taking oral potassium supplementation; the figures in the APA and non-PA groups were 73.9 and 15.0%, respectively.

ACTH stimulation test under dexamethasone suppression

We analyzed the results of the ACTH stimulation tests under 1-mg dexamethasone suppression in all 59 patients to investigate its accuracy in the differential diagnosis of IHA, APA, and non-PA groups. The mean PAC values of the IHA, APA, and non-PA groups before ACTH injection (PAC_{0min}) were 11.6, 17.1, and 11.1 ng/dl, respectively. The PAC_{0min} value in the APA group tended to be higher than those in the IHA and non-PA groups, but the differences were not significant. PAC values rose in all groups after ACTH stimulation. In the IHA group, the mean PAC_{30min}, PAC_{60min}, PAC_{90min}, and PAC_{120min} values were 33.0, 34.6, 31.9, and 27.8 ng/dl, respectively (Fig. 2A). In the APA group, the mean PAC_{30min}, PAC_{60min}, PAC_{90min}, and PAC_{120min} values were 64.7, 80.1, 75.2, and 62.6 ng/dl, respectively (Fig. 2A). In the non-PA group, the mean PAC_{30min}, PAC_{60min}, PAC_{90min}, and PAC_{120min} values were 32.4, 34.4, 32.2, and 27.0 ng/dl, respectively. The fold increase from PAC_{0min} after ACTH injection (PAC_{30min}/PAC_{0min}, PAC_{60min}/PAC_{0min}, PAC_{90min}/PAC_{0min}, and PAC_{120min}/PAC_{0min}) in the IHA and APA groups are shown in Fig. 2B. After ACTH stimulation, the PAC values of the APA group were significantly higher than those in the IHA and non-PA groups at all data points. Figure 3 shows the plots of PAC values of each group before and after ACTH stimulation.

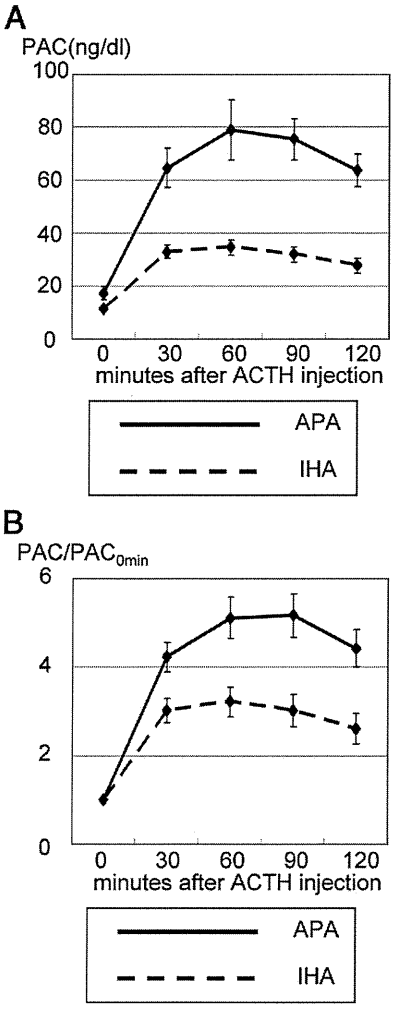

FIG. 2. PAC values (A) and PAC_{0min}-corrected PAC values (B), before (0 min) and after (30, 60, 90, 120 min) ACTH injections of IHA group (*dashed line*), and APA group (*continuous line*). Data are shown as means ± SEM.

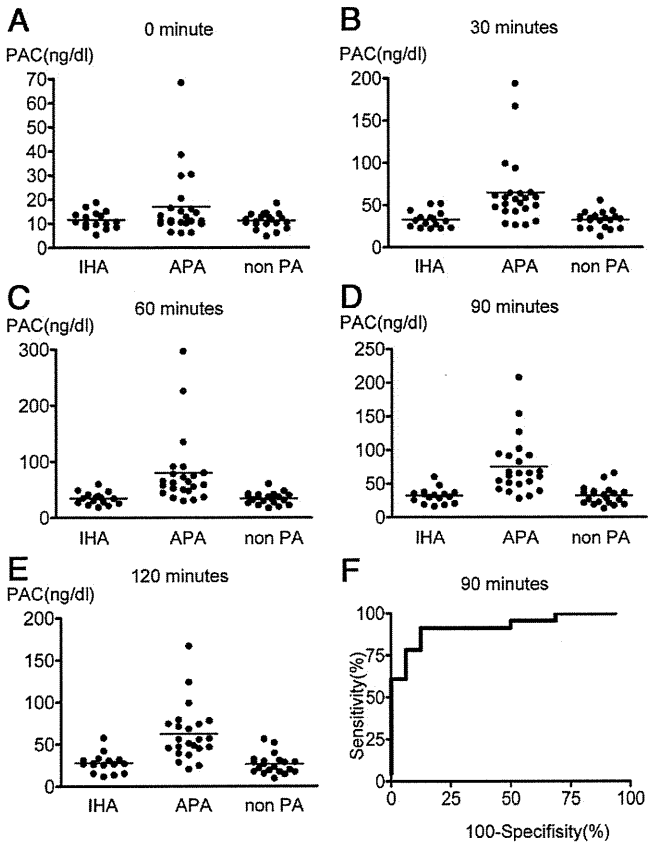

FIG. 3. A–E, Scattergram of PAC values of non-PA, IHA, and APA group before (A), and 30 min (B), 60 min (C), 90 min (D), and 120 min (E) after the ACTH injection. F, ROC curve of PAC values 90 min after the ACTH injection in the differential diagnosis between IHA and APA.

Diagnostic accuracy of ACTH stimulation test in the diagnosis of an APA

We first analyzed the diagnostic accuracy of ACTH stimulation test in the differential diagnosis between IHA and an APA. Table 2 shows the results of ROC curve analysis of PAC values for each time point after ACTH stimulation. At all time points, the AUC was higher than that under the diagonal, indicating that the PAC values for 30, 60, 90, and 120 min after ACTH stimulation were all useful in the differential diagnosis between the APA and IHA groups. The AUC was highest at 90 min after ACTH stimulation, and the optimal cutoff value of the PAC for the diagnosis of an APA was greater than 37.9 ng/dl. These results corresponded with sensitivity and specificity of 91.3 and 87.5%, respectively.

Next, we analyzed the diagnostic accuracy of the ACTH stimulation test in the diagnosis of an APA among IHA, APA, and non-PA patients. Table 2 shows the results of the ROC curve analysis for PAC values at each time point after ACTH stimulation. At every time point, the AUC was higher than that under the diagonal, indicating that the PAC values 30, 60, 90, and 120 min after ACTH stimulation were all useful in the diagnosis of an APA. The AUC was highest at 90 min after ACTH stimulation, and the optimal cutoff value of the PAC for the diagnosis of an APA was greater than 37.9 ng/dl. These data correspond with sensitivity and specificity of 91.3 and 80.6%, respectively.

To investigate whether the fold increase from PAC_{0min} after ACTH stimulation could improve the diagnostic accuracy over the raw PAC value, we measured the AUC under ROC curve of the fold increase from PAC_{0min} after ACTH stimulation. We found that the fold increase from PAC_{0min} worsens the diagnostic accuracy at any time point after ACTH stimulation (data not shown).

Discussion

The high prevalence of PA among hypertensive patients and the potential need for surgery in those with an APA

TABLE 2. Results of the ROC curve analysis of PAC values before and after ACTH stimulation

Time point	AUC (95% CI)	Optimal cutoff (ng/dl)	Sensitivity at optimal cutoff (%)	Specificity at optimal cutoff (%)
Diagnosis of APA group between APA and IHA groups				
Before	0.622 (0.443 to 0.801)	>11.0	65.2	56.3
30 min	0.851 (0.731 to 0.970)	>41.5	82.6	81.3
60 min	0.889 (0.788 to 0.989)	>47.3	78.3	87.5
90 min	0.921 (0.836 to 1.007)	>37.9	91.3	87.5
120 min	0.883 (0.771 to 0.995)	>35.3	87.0	87.5
Diagnosis of APA group among IHA, APA, and non-PA groups				
Before	0.623 (0.472 to 0.775)	>12.9	47.8	69.4
30 min	0.855 (0.745 to 0.965)	>42.2	82.6	86.1
60 min	0.885 (0.794 to 0.976)	>43.6	82.6	86.1
90 min	0.913 (0.838 to 0.988)	>37.9	91.3	80.6
120 min	0.889 (0.800 to 0.978)	>35.3	87.0	86.1

CI, Confidence interval.

make effective detection of PA an important issue. Subtype diagnosis of PA requires a costly procedure that is not always accessible. Taking into consideration the high prevalence of PA among hypertensive patients, it is practically impossible to perform confirmatory subclass diagnostic procedures, such as AVS, for all the patients with confirmed PA because these procedures are currently limited to large medical centers. Therefore, a simpler and more accessible procedure is required to select patients who are highly suspicious of an APA and definitely need confirmatory subclass diagnostic procedures.

The posture stimulation test, which was formerly used to distinguish between an APA and IHA (23, 24), proved to have a low diagnostic accuracy (30, 31), probably because of the considerable percentage of AII-R APA, which are indistinguishable from IHA by the test, among all APA (27).

Meanwhile, PAC in the cases of AII-R APA were reported to also be responsive to ACTH stimulation (28). Stowasser *et al.* (28) found that the PAC of AII-R APA patients during ACTH infusion were similar to, or even higher than, those of AII-U APA patients, although the PAC of IHA patients during ACTH infusion were significantly lower than those of AII-R APA and AII-U APA patients. This report suggests that ACTH stimulation is useful in the differential diagnosis between an APA and IHA because PAC of both AII-R APA and APA-U APA patients are more responsive to ACTH than in IHA patients.

The idea of the ACTH stimulation test under dexamethasone suppression was first published by Kem *et al.* (34) in 1978. In that report, there was a difference in PAC in response to ACTH between APA and IHA patients under certain circumstances. However, the diagnostic accuracy of this test in differentiating an APA and IHA was not evaluated. In our study, we demonstrated that the ACTH stimulation test under dexamethasone suppression is highly sensitive for distinguishing patients with an APA from those with IHA or non-PA.

Our study is based on the prior observation that an APA is generally more sensitive to ACTH than IHA or essential hypertension, probably owing to the expression of ACTH receptors on an APA (35). Similar to APA cases, several reports show that in some cases of IHA, PAC respond well to ACTH stimulation (32). This study included such cases. In two patients in the IHA group, PAC values at 90 min after ACTH stimulation were higher than 37.9 ng/dl. However, as shown in our ROC curve analyses, we could identify patients highly suspected of having an APA among those suspected of PA with high sensitivity. Although this test cannot be used for final diagnosis of an APA, it can be used to screen patients who are highly suspected of having an APA and definitely need AVS.

In the present study, we hypothesized that 1-mg dexamethasone suppression would result in a greater decrease in PAC_{0min} in the ACTH-sensitive APA group compared with IHA and non-PA patients and that the fold increase from PAC_{0min} after ACTH stimulation would provide more accurate diagnostic criteria than raw PAC values. However, to our surprise, the latter proved more useful according to the ROC curve analysis. This is partly because the PAC_{0min} values were higher in APA patients than non-PA and IHA patients despite the dexamethasone suppression. Further studies are needed to clarify whether dexamethasone suppression is necessary in this ACTH stimulation test.

In this study, we made the decision of the lateralization of aldosterone hypersecretion with LR and CLR in AVS after ACTH stimulation. However, when performing AVS, we always obtain blood samples from both adrenal veins and inferior vena cava before and after ACTH stimulation to avoid sampling errors. Applying the same criterion for lateralization as AVS with ACTH stimulation (LR >3 and CLR ≤ 1 for unilateral aldosterone hypersecretion; and LR ≤ 3 and CLR >1 for bilateral aldosterone hypersecretion) to AVS without ACTH stimulation (36), two of 23 patients in the APA group were diagnosed with bilateral aldosterone hypersecretion by AVS without ACTH stimulation, and two of 16 patients in the IHA group were diagnosed with unilateral aldosterone hypersecretion by AVS without ACTH stimulation. The PAC of

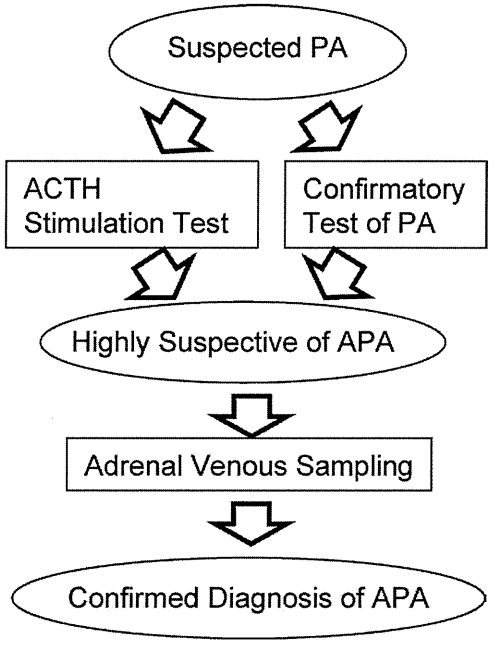

FIG. 4. A diagnostic flowchart that we suggest in the diagnosis of an APA.

the two patients in the APA group who were diagnosed with bilateral aldosterone hypersecretion by AVS without ACTH stimulation responded well to the ACTH stimulation test. They underwent laparoscopic adrenalectomy and were histologically proven to have had an adrenal adenoma. After adrenalectomy, their hypertension and hypokalemia were cured. In two patients in the IHA group diagnosed with unilateral aldosterone hypersecretion by AVS without ACTH stimulation, no adrenal tumor was detected on CT scanning, although histological diagnosis could not be made. They were treated medically with aldosterone receptor blockers. Our results do not agree with a previous study by Seccia *et al.* (37), which showed that ACTH stimulation during AVS is confounding for diagnosis of an APA. However, Seccia *et al.* (37) used a selectivity index cutoff (>1.1) that was shown to be unreliable by others (36, 38, 39), justifying caution for the validity of their findings.

Earlier studies found that PAC levels in IHA patients are usually higher than those in essential hypertension patients. In this study, as shown in Table 1 and Fig. 3, the baseline PAC did not differ between the IHA group and the non-PA group. All patients in this study met the screening criteria of ARR greater than 20 at least once in an outpatient setting. Thus, most of those in the non-PA group had low renin hypertension, and they were substantially different from common essential hypertension patients. Moreover, the accurate diagnostic criteria for IHA have yet to be defined. Some reports consider it the part of PA not diagnosed as APA, whereas others regard it as bilateral aldosterone secretion. Pathologically, IHA is defined as hyperplasia of zona glomerulosa that hypersecrete aldosterone. However, most patients with IHA do not undergo surgery, and pathology-based diagnosis of IHA is rare. Therefore, the differential diagnosis between IHA and non-PA hypertension is usually based on the confirmatory diagnostic tests for PA. However, these tests do not always clearly discriminate between patients with PA and those without it. Rossi *et al.* (40) found that the AUC for diagnosis of PA by the saline infusion and captopril challenge tests were relatively low (0.811 and 0.785, respectively). Therefore, the non-PA group in the present study may have included IHA patients, and vice versa. However, the aim of this study was to detect patients highly suspicious of an APA that called for a definitive diagnostic test of PA subtype. The difference is important because an APA can be cured by surgery, and both essential hypertension and IHA benefit from medical treatments.

Our study is limited by its retrospective nature. A prospective, large-scale study is required to confirm the diagnostic accuracy of the rapid ACTH stimulation test under dexamethasone suppression in the diagnosis of an APA.

In conclusion, this study shows that the ACTH stimulation test is a supportive procedure in the diagnosis of an APA among patients suspected of PA. Although this test was not definitive enough for the final diagnosis of an APA, it can be performed in an outpatient setting and does not require special technique or devices. We rather suggest using this test to select candidates for a definitive subtype diagnostic test among those with suspected or confirmed PA (Fig. 4).

Acknowledgments

We gratefully acknowledge the support of nursing, laboratory, and secretarial staff in our department and the medical staff in the departments of urology, radiology, and pathology of the Kyoto University Hospital.

Address all correspondence and requests for reprints to: Masakatsu Sone, M.D., Ph.D., Department of Medicine and Clinical Science, Kyoto University Graduate School of Medicine, 54 Shogoin Kawahara-cho, Sakyo-ku, Kyoto 606-8507, Japan. E-mail: sonemasa@kuhp.kyoto-u.ac.jp.

This work was supported by Grants-in-Aid for research on intractable disease from the Ministry of Healthy, Labour, and Welfare.

Disclosure Summary: The authors have nothing to disclose.

References

1. Rossi GP, Bernini G, Caliumi C, Desideri G, Fabris B, Ferri C, Ganzaroli C, Giacchetti G, Letizia C, Maccario M, Mallamaci F, Mannelli M, Mattarello MJ, Moretti A, Palumbo G, Parenti G, Porteri E, Semplicini A, Rizzoni D, Rossi E, Boscaro M, Pessina AC, Mantero F; PAPY Study Investigators 2006 A prospective study of the prevalence of primary aldosteronism in 1125 hypertensive patients. J Am Coll Cardiol 48:2293–2300
2. Fardella CE, Mosso L, Gómez-Sánchez C, Cortés P, Soto J, Gómez L, Pinto M, Huete A, Oestreicher E, Foradori A, Montero J 2000 Primary aldosteronism in essential hypertensives: prevalence, biochemical profile, and molecular biology. J Clin Endocrinol Metab 85:1863–1867
3. Mulatero P, Dluhy RG, Giacchetti G, Boscaro M, Veglio F, Stewart PM 2005 Diagnosis of primary aldosteronism: from screening to subtype differentiation. Trends Endocrinol Metab 16:114–119
4. Loh KC, Koay ES, Khaw MC, Emmanuel SC, Young Jr WF 2000 Prevalence of primary aldosteronism among Asian hypertensive patients in Singapore. J Clin Endocrinol Metab 85:2854–2859
5. Fogari R, Preti P, Zoppi A, Rinaldi A, Fogari E, Mugellini A 2007 Prevalence of primary aldosteronism among unselected hypertensive patients: a prospective study based on the use of an aldosterone/renin ratio above 25 as a screening test. Hypertens Res 30:111–117
6. Omura M, Saito J, Yamaguchi K, Kakuta Y, Nishikawa T 2004 Prospective study on the prevalence of secondary hypertension among hypertensive patients visiting a general outpatient clinic in Japan. Hypertens Res 27:193–202
7. Milliez P, Girerd X, Plouin PF, Blacher J, Safar ME, Mourad JJ 2005 Evidence for an increased rate of cardiovascular events in patients with primary aldosteronism. J Am Coll Cardiol 45:1243–1248
8. Catena C, Colussi G, Lapenna R, Nadalini E, Chiuch A, Gianfagna P, Sechi LA 2007 Long-term cardiac effects of adrenalectomy or

mineralocorticoid antagonists in patients with primary aldosteronism. Hypertension 50:911–918
9. Sechi LA, Novello M, Lapenna R, Baroselli S, Nadalini E, Colussi GL, Catena C 2006 Long-term renal outcomes in patients with primary aldosteronism. JAMA 295:2638–2645
10. Rossi GP, Bernini G, Desideri G, Fabris B, Ferri C, Giacchetti G, Letizia C, Maccario M, Mannelli M, Matterello MJ, Montemurro D, Palumbo G, Rizzoni D, Rossi E, Pessina AC, Mantero F; PAPY Study Participants. 2006 Renal damage in primary aldosteronism: results of the PAPY Study. Hypertension 48:232–238
11. Funder JW, Carey RM, Fardella C, Gomez-Sanchez CE, Mantero F, Stowasser M, Young Jr WF, Montori VM 2008 Case detection, diagnosis, and treatment of patients with primary aldosteronism: an Endocrine Society Clinical Practice Guideline. J Clin Endocrinol Metab 93:3266–3281
12. Ogihara T, Kikuchi K, Matsuoka H, Fujita T, Higaki J, Horiuchi M, Imai Y, Imaizumi T, Ito S, Iwao H, Kario K, Kawano Y, Kim-Mitsuyama S, Kimura G, Matsubara H, Matsuura H, Naruse M, Saito I, Shimada K, Shimamoto K, Suzuki H, Takishita S, Tanahashi N, Tsuchihashi T, Uchiyama M, Ueda S, Ueshima H, Umemura S, Ishimitsu T, Rakugi H; Japanese Society of Hypertension Committee 2009 The Japanese Society of Hypertension Guidelines for the Management of Hypertension (JSH 2009). Hypertens Res 32:3–107
13. Lyons DF, Kem DC, Brown RD, Hanson CS, Carollo ML 1983 Single dose captopril as a diagnostic test for primary aldosteronism. J Clin Endocrinol Metab 57:892–896
14. Holland OB, Brown H, Kuhnert L, Fairchild C, Risk M, Gomez-Sanchez CE 1984 Further evaluation of saline infusion for the diagnosis of primary aldosteronism. Hypertension 6:717–723
15. Agharazii M, Douville P, Grose JH, Lebel M 2001 Captopril suppression versus salt loading in confirming primary aldosteronism. Hypertension 37:1440–1443
16. Streeten DH, Tomycz N, Anderson GH 1979 Reliability of screening methods for the diagnosis of primary aldosteronism. Am J Med 67:403–413
17. Young WF 2007 Primary aldosteronism: renaissance of a syndrome. Clin Endocrinol (Oxf) 66:607–618
18. Magill SB, Raff H, Shaker JL, Brickner RC, Knechtges TE, Kehoe ME, Findling JW 2001 Comparison of adrenal vein sampling and computed tomography in the differentiation of primary aldosteronism. J Clin Endocrinol Metab 86:1066–1071
19. Young WF, Stanson AW, Thompson GB, Grant CS, Farley DR, van Heerden JA 2004 Role for adrenal venous sampling in primary aldosteronism. Surgery 136:1227–1235
20. Young WF, Stanson AW 2009 What are the keys to successful adrenal venous sampling (AVS) in patients with primary aldosteronism? Clin Endocrinol (Oxf) 70:14–17
21. Nomura K, Kusakabe K, Maki M, Ito Y, Aiba M, Demura H 1990 Iodomethylnorcholesterol uptake in an aldosteronoma shown by dexamethasone-suppression scintigraphy: relationship to adenoma size and functional activity. J Clin Endocrinol Metab 71:825–830
22. Mansoor GA, Malchoff CD, Arici MH, Karimeddini MK, Whalen GF 2002 Unilateral adrenal hyperplasia causing primary aldosteronism: limitations of I-131 norcholesterol scanning. Am J Hypertens 15:459–464
23. Schambelan M, Brust NL, Chang BC, Slater KL, Biglieri EG 1976 Circadian rhythm and effect of posture on plasma aldosterone concentration in primary aldosteronism. J Clin Endocrinol Metab 43:115–131
24. Biglieri EG 1991 Spectrum of mineralocorticoid hypertension. Hypertension 17:251–261
25. Wisgerhof M, Carpenter PC, Brown RD 1978 Increased adrenal sensitivity to angiotensin II in idiopathic hyperaldosteronism. J Clin Endocrinol Metab 47:938–943
26. Wisgerhof M, Brown RD, Hogan MJ, Carpenter PC, Edis AJ 1981 The plasma aldosterone response to angiotensin II infusion in aldosterone-producing adenoma and idiopathic hyperaldosteronism. J Clin Endocrinol Metab 52:195–198
27. Tunny TJ, Klemm SA, Stowasser M, Gordon RD 1993 Angiotensin-responsive aldosterone-producing adenomas: postoperative disappearance of aldosterone response to angiotensin. Clin Exp Pharmacol Physiol 20:306–309
28. Stowasser M, Klemm SA, Tunny TJ, Gordon RD 1995 Plasma aldosterone response to ACTH in subtypes of primary aldosteronism. Clin Exp Pharmacol Physiol 22:460–462
29. Stowasser M, Bachmann AW, Tunny TJ, Gordon RD 1996 Production of 18-oxo-cortisol in subtypes of primary aldosteronism. Clin Exp Pharmacol Physiol 23:591–593
30. Phillips JL, Walther MM, Pezzullo JC, Rayford W, Choyke PL, Berman AA, Linehan WM, Doppman JL, Gill Jr JR 2000 Predictive value of preoperative tests in discriminating bilateral adrenal hyperplasia from an aldosterone-producing adrenal adenoma. J Clin Endocrinol Metab 85:4526–4533
31. Sheaves R, Goldin J, Reznek RH, Chew SL, Dacie JE, Lowe DG, Ross RJ, Wass JA, Besser GM, Grossman AB 1996 Relative value of computed tomography scanning and venous sampling in establishing the cause of primary hyperaldosteronism. Eur J Endocrinol 134:308–313
32. Biglieri EG, Irony I, Kater CE 1989 Identification and implications of new types of mineralocorticoid hypertension. J Steroid Biochem 32:199–204
33. Yamahara K, Itoh H, Yamamoto A, Sasano H, Masatsugu K, Sawada N, Fukunaga Y, Sakaguchi S, Sone M, Yurugi T, Nakao K 2002 New diagnostic procedure for primary aldosteronism: adrenal venous sampling under adrenocorticotropic hormone and angiotensin II receptor blocker—application to a case of bilateral multiple adrenal microadenomas. Hypertens Res 25:145–152
34. Kem DC, Weinberger MH, Higgins JR, Kramer NJ, Gomez-Sanchez C, Holland OB 1978 Plasma aldosterone response to ACTH in primary aldosteronism and in patients with low renin hypertension. J Clin Endocrinol Metab 46:552–560
35. Reincke M, Beuschlein F, Latronico AC, Arlt W, Chrousos GP, Allolio B 1997 Expression of adrenocorticotrophic hormone receptor mRNA in human adrenocortical neoplasms: correlation with P450scc expression. Clin Endocrinol (Oxf) 46:619–626
36. Mulatero P, Bertello C, Sukor N, Gordon R, Rossato D, Daunt N, Leggett D, Mengozzi G, Veglio F, Stowasser M 2010 Impact of different diagnostic criteria during adrenal vein sampling on reproducibility of subtype diagnosis in patients with primary aldosteronism. Hypertension 55:667–673
37. Seccia TM, Miotto D, De Toni R, Pitter G, Mantero F, Pessina AC, Rossi GP 2009 Adrenocorticotropic hormone stimulation during adrenal vein sampling for identifying surgically curable subtypes of primary aldosteronism: comparison of 3 different protocols. Hypertension 53:761–766
38. Solar M, Ceral J, Krajina A, Ballon M, Malirova E, Brodak M, Cap J 2010 Adrenal venous sampling: where is the aldosterone disappearing to? Cardiovasc Intervent Radiol 33:760–765
39. Ceral J, Solar M, Krajina A, Ballon M, Suba P, Cap J 2010 Adrenal venous sampling in primary aldosteronism: a low dilution of adrenal venous blood is crucial for a correct interpretation of the results. Eur J Endocrinol 162:101–107
40. Rossi GP, Belfiore A, Bernini G, Desideri G, Fabris B, Ferri C, Giacchetti G, Letizia C, Maccario M, Mallamaci F, Mannelli M, Palumbo G, Rizzoni D, Rossi E, Agabiti-Rosei E, Pessina AC, Mantero F; Primary Aldosteronism Prevalence in Italy Study Investigators 2007 Comparison of the captopril and the saline infusion test for excluding aldosterone-producing adenoma. Hypertension 50:424–431

Angiogenic and Vasoprotective Effects of Adrenomedullin on Prevention of Cognitive Decline After Chronic Cerebral Hypoperfusion in Mice

Takakuni Maki, MD; Masafumi Ihara, MD, PhD; Youshi Fujita, MD, PhD; Takuo Nambu, MD, PhD; Kazutoshi Miyashita, MD, PhD; Mahito Yamada, MD; Kazuo Washida, MD; Keiko Nishio, MD; Hidefumi Ito, MD, PhD; Hiroshi Harada, PhD; Hideki Yokoi, MD, PhD; Hiroshi Arai, MD, PhD; Hiroshi Itoh, MD, PhD; Kazuwa Nakao, MD, PhD; Ryosuke Takahashi, MD, PhD; Hidekazu Tomimoto, MD, PhD

Background and Purpose—Although subcortical vascular dementia, the major subtype of vascular dementia, is caused by a disruption in white matter integrity after cerebrovascular insufficiency, no therapy has been discovered that will restore cerebral perfusion or functional cerebral vessels. Because adrenomedullin (AM) has been shown to be angiogenic and vasoprotective, the purpose of the study was to investigate whether AM may be used as a putative treatment for subcortical vascular dementia.

Methods—A model of subcortical vascular dementia was reproduced in mice by placing microcoils bilaterally on the common carotid arteries. Using mice overexpressing circulating AM, we assessed the effect of AM on cerebral perfusion, cerebral angioarchitecture, oxidative stress, white matter change, cognitive function, and brain levels of cAMP, vascular endothelial growth factor, and basic fibroblast growth factor.

Results—After bilateral common carotid artery stenosis, mice overexpressing circulating AM showed significantly faster cerebral perfusion recovery due to substantial growth of the capillaries, the circle of Willis, and the leptomeningeal anastomoses and reduced oxidative damage in vascular endothelial cells compared with wild-type mice. Vascular changes were preceded by upregulation of cAMP, vascular endothelial growth factor, and basic fibroblast growth factor. White matter damage and working memory deficits induced by bilateral common carotid artery stenosis were subsequently restored in mice overexpressing circulating AM.

Conclusions—These data indicate that AM promotes arteriogenesis and angiogenesis, inhibits oxidative stress, preserves white matter integrity, and prevents cognitive decline after chronic cerebral hypoperfusion. Thus, AM may serve as a strategy to tackle subcortical vascular dementia. **(*Stroke*. 2011;42:1122-1128.)**

Key Words: angiogenesis ■ arteriogenesis ■ adrenomedullin ■ vascular dementia

Ischemic white matter (WM) lesions, which are most likely caused by cerebrovascular insufficiency after atherosclerosis and/or arteriosclerosis, are an established marker of risk for cognitive deterioration.[1] Thus, therapeutic vascular growth and vasoprotection, resulting in the preservation of WM integrity, may serve to maintain cognitive function in subjects at risk of developing dementia.

Adrenomedullin (AM) has a variety of effects on the vasculature that include vasodilation, regulation of permeability, inhibition of endothelial cell apoptosis and oxidative stress, regulation of smooth muscle cell proliferation, and promotion of angiogenesis.[2,3]

Thus, the purpose of this study was to investigate the mechanisms and therapeutic potential of AM-induced neovascularization and/or vasoprotection after chronic cerebral hypoperfusion in a mouse model of subcortical vascular dementia.[4,5]

Materials and Methods

An expanded Methods section is available in the Online Data Supplement (http://stroke.ahajournals.org).

Results

Adrenomedullin Facilitates Recovery of Cerebral Blood Flow After Placing Microcoils Bilaterally on the Common Carotid Arteries

Immediately after bilateral common carotid artery stenosis (BCAS), cerebral blood flow (CBF) decreased to the lowest

Received September 22, 2010; final revision received November 11, 2010; accepted November 15, 2010.

From the Departments of Neurology (T.M., M.I., Y.F., M.Y., K.W., K. Nishio, K. Ito, R.T.), Medicine and Clinical Science (T.N., H.Y., H.A., K. Nakao), and Radiation Oncology and Image-applied Therapy (H.H.), Graduate School of Medicine, Kyoto University, Kyoto, Japan; the Department of Internal Medicine (K.M., H. Itoh), Graduate School of Medicine, Keio University, Tokyo, Japan; and the Department of Neurology (H.T.), Graduate School of Medicine, Mie University, Mie, Japan.

The online-only Data Supplement is available at http://stroke.ahajournals.org/cgi/content/full/STROKEAHA.110.603399/DC1.

Correspondence to Masafumi Ihara, MD, PhD, Department of Neurology, Graduate School of Medicine, Kyoto University, Shogoin, Sakyo-ku, Kyoto 606-8507, Japan. E-mail ihara@kuhp.kyoto-u.ac.jp

Stroke is available at http://stroke.ahajournals.org DOI: 10.1161/STROKEAHA.110.603399

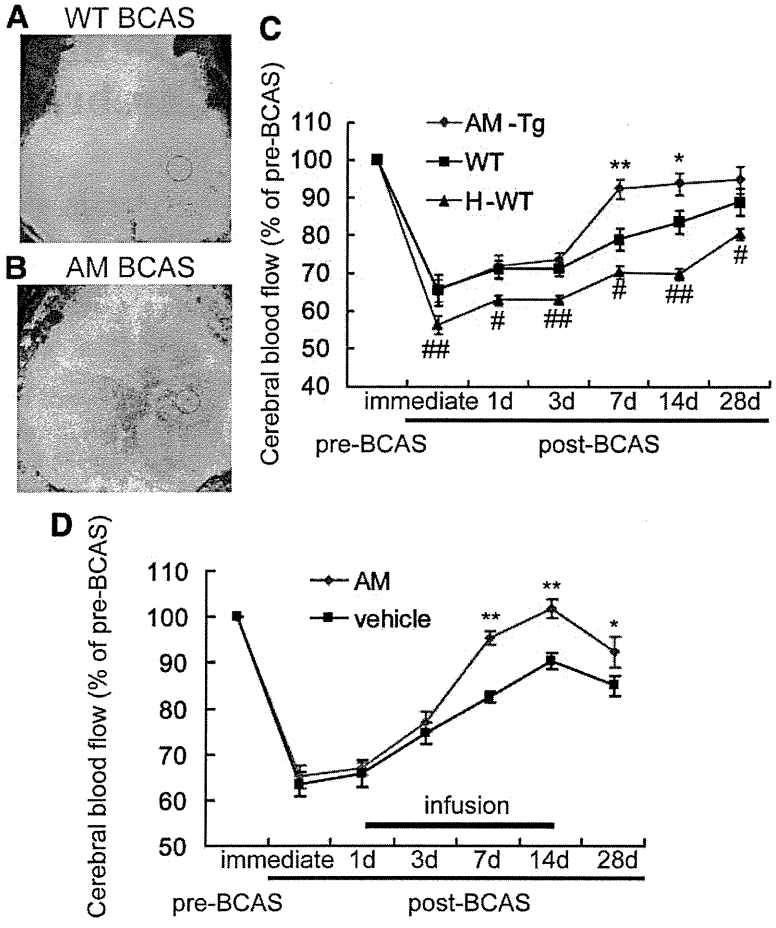

Figure 1. Adrenomedullin (AM) facilitates recovery of cerebral blood flow after the bilateral common carotid artery stenosis (BCAS). A–B, Representative images of CBF in wild-type or AM-Tg mouse subjected to BCAS operation (WT BCAS or AM BCAS) on Day 7. C, Temporal profile of CBF after BCAS in wild-type (WT; n=16 on Days 0 to 14, n=8 on Day 28), AM-Tg (n=16 on Days 0 to 14, n=8 on Day 28), and hydralazine-treated WT (H-WT; n=8 on Days 0 to 14, n=4 on Day 28) mice, in which the pre-BCAS value of CBF is adjusted to 100. Values are expressed as means±SEM. *P<0.05, **P<0.01 in AM-Tg vs WT; #P<0.05, ##P<0.01 in WT vs H-WT. D, Temporal profile of CBF after BCAS in AM-treated WT mice (n=11) and vehicle-treated WT mice (n=10). Values are expressed as means±SEM *P<0.05, **P<0.01. CBF indicates cerebral blood flow; AM-Tg, mice overexpressing circulating AM.

values but thereafter began to recover in all groups. On Days 1 and 3 post-BCAS, there was a slight, but not significant, increase in CBF (average±SEM) in mice overexpressing circulating AM (AM-Tg) compared with wild-type (WT) mice. On Day 7 post-BCAS, AM-Tg mice showed significantly faster CBF recovery: CBF was significantly higher in AM-Tg mice (93%±2%) compared with WT mice (79%±2%) and hydralazine-treated WT mice (71%±2%; Figure 1A–C). This trend continued on Days 14 and 28 post-BCAS (Figure 1C; Supplemental Figure IA). Slower CBF recovery in hydralazine-treated WT mice suggests that AM-induced CBF recovery may not be associated with the hypotensive effect of AM.

We further examined the effects of postoperative exogenous infusion of AM.[6,7] Continuous intraperitoneal injection of recombinant human AM at a rate of 50 ng/hr for 2 weeks, beginning on Day 1 post-BCAS, resulted in a significantly faster CBF recovery compared with the vehicle-treated mice (Figure 1D). These effects were comparable to those seen in BCAS-operated AM-Tg mice.

Thus, both genetically overproduced AM and postoperative exogenous administration of AM facilitated recovery of CBF after BCAS.

Adrenomedullin Enhances Arteriogenesis After BCAS

At the dorsal surface of the brain, a significant increase in diameter of the leptomeningeal anastomoses was found in AM-Tg mice (28.7±1.6 μm) compared with WT mice (22.4±1.3 μm) on Day 7 post-BCAS (Figure 2A–C; Supplemental Figure IB, a–d). The number of leptomeningeal anastomoses was not different among the 4 groups. The diameter of the internal carotid artery, anterior cerebral artery, middle cerebral artery, and posterior communicating artery was significantly enlarged at the level of the circle of Willis in AM-Tg mice compared with WT mice (AM-Tg versus WT; anterior cerebral artery, 193±26 versus 161±24 μm; middle cerebral artery, 184±24 versus 153±13 μm; internal carotid artery, 206±30 versus 175±25 μm; posterior communicating artery, 191±16 versus 150±15 μm) on Day 7 post-BCAS (Figure 2D; Supplemental Figure IB, e–h).

To evaluate monocyte recruitments and proliferation of smooth muscle cells, both of which are essential in arteriogenesis, the immunofluorescent analysis of Ki-67 and F4/80, together with α-smooth muscle actin, was performed. BCAS-operated AM-Tg mice showed a significant increase in Ki-67-positive vascular smooth muscle cells compared with BCAS-operated WT mice (Supplemental Figure IC). In addition, a significant increase in vascular smooth muscle cells surrounded by F4/80-positive monocyte/macrophages was found in BCAS-operated AM-Tg mice compared with sham-operated WT mice (Supplemental Figure ID).

Adrenomedullin Enhances Angiogenesis After BCAS

A significant increase in platelet-endothelial cell adhesion molecule-1-positive capillary density of the cortex, corpus cal-

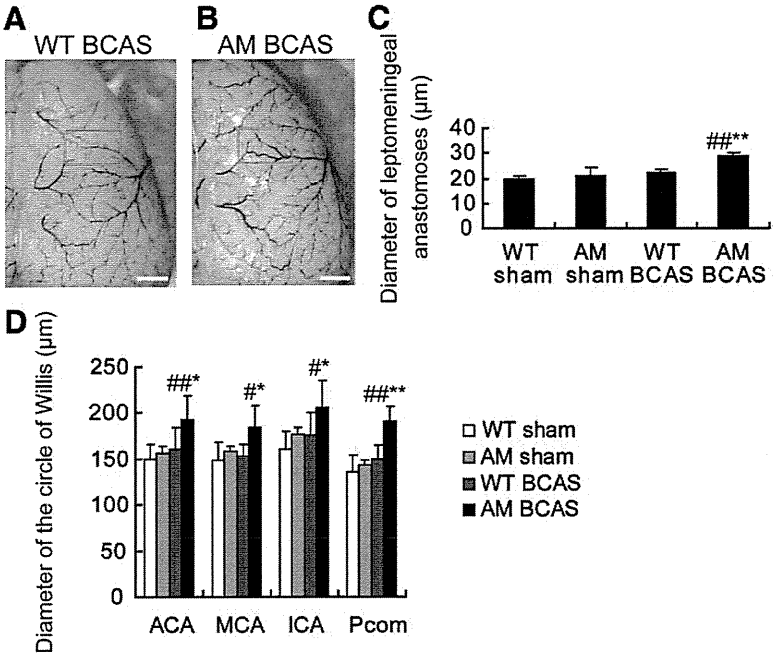

Figure 2. Adrenomedullin (AM) enhances arteriogenesis after BCAS. A–B, Representative images of the dorsal cerebral angioarchitecture by postmortem latex perfusion method of wild-type (WT) or AM-Tg mouse subjected to BCAS operation (WT BCAS or AM BCAS) on day 7. Scale bars, 1 mm. C–D, Histogram showing the diameter of the leptomeningeal anastomoses (C) and the anterior, middle, and posterior cerebral arteries (ACA, MCA, and PCA, respectively) and the posterior communicating artery (Pcom; D) of WT or AM-Tg mouse subjected to sham or BCAS operation on Day 7 (WT sham, n=4; AM sham, n=4; WT BCAS, n=6; AM BCAS, n=6). Error bars indicate SD. *P<0.05, **P<0.01 in AM BCAS vs WT BCAS; #P<0.05, ##P<0.01 vs WT sham. BCAS indicates bilateral common carotid artery stenosis; AM-Tg, mice overexpressing circulating AM.

losum, and caudoputamen was found in AM-Tg mice compared with WT mice (AM-Tg versus WT; cortex, 540±55/mm^2 versus 473±38/mm^2; corpus callosum, 273±7/mm^2 versus 213±18/mm^2; caudoputamen, 499±36/mm^2 versus 455±26/mm^2) on Day 7 post-BCAS. There was no significant difference in capillary density between AM-Tg and WT mice after sham operation (Figure 3A–C; Supplemental Figure IE).

Taken together, these results suggest that both chronic ischemic stress and AM overexpression are required to induce arteriogenesis and angiogenesis in the brain.

Adrenomedullin Attenuates Oxidative Damage in Cerebral Microvessels After BCAS

To evaluate oxidative damage in cerebral microvessels, double immunofluorescence staining for platelet-endothelial cell adhesion molecule-1 and 8-hydroxy-deoxyguanosine was performed on Day 3 post-BCAS. A significant decrease in oxidative damage in the cerebral microvessels was found in BCAS-operated AM-Tg mice compared with BCAS-operated WT mice (Figure 3D; Supplemental Figure IF).

Adrenomedullin Preserves WM Integrity After BCAS

BCAS-operated WT mice showed an increased density of glial fibrillary acidic protein-positive astrocytes and ionized calcium binding adapter molecule 1-positive microglia and a decreased density of glutathione-S-transferase-pi-immunoreactive mature oligodendrocytes in the corpus callosum and the anterior commissure compared with sham-operated WT or AM-Tg

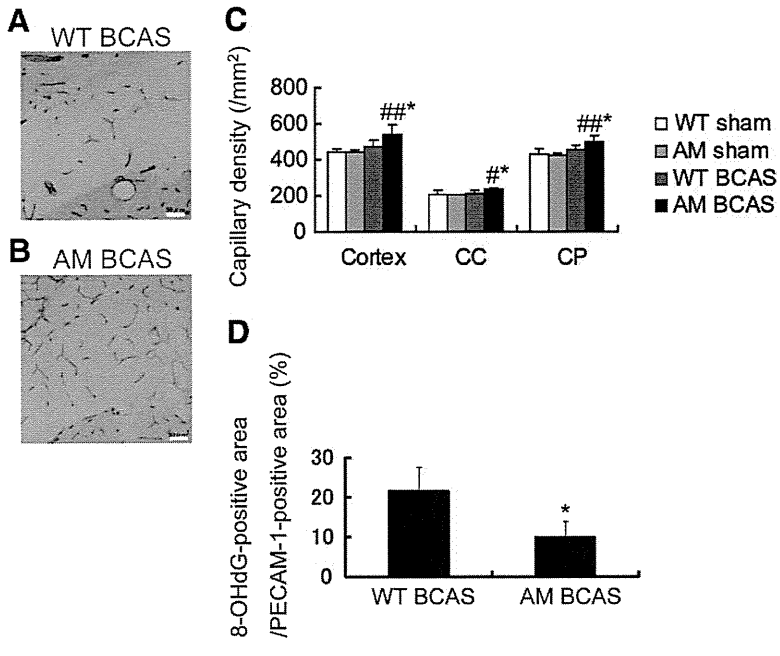

Figure 3. Adrenomedullin (AM) enhances angiogenesis and attenuates oxidative damage in brain microvessels after BCAS. A–B, Representative images of PECAM-1-positive capillaries in corpus callosum sections of a wild-type (WT) or AM-Tg mouse subjected to BCAS operation (WT BCAS or AM BCAS) on Day 7. Scale bar, 50 μm. C, Histogram showing capillary densities of the cortex, corpus callosum (CC), and caudoputamen (CP) of WT or AM-Tg mouse that is subjected to sham or BCAS operation on Day 7 (WT sham, n=4; AM sham, n=4; WT BCAS, n=6; AM BCAS, n=6). Error bars indicate SD. *P<0.05 in AM BCAS vs WT BCAS; #P<0.05, ##P<0.01 vs WT sham. D, To evaluate oxidative damage in cerebral microvessels, double immunofluorescence staining for PECAM-1 and 8-hydroxy-deoxyguanosine (8-OHdG) was performed. Histogram showing oxidative damage in microvessels of the corpus callosum of WT BCAS or AM BCAS (n=4 each). Error bars indicate SD. *P<0.05 vs WT BCAS. BCAS indicates bilateral common carotid artery stenosis; PECAM-1, platelet-endothelial cell adhesion molecule-1; AM-Tg, mice overexpressing circulating AM.

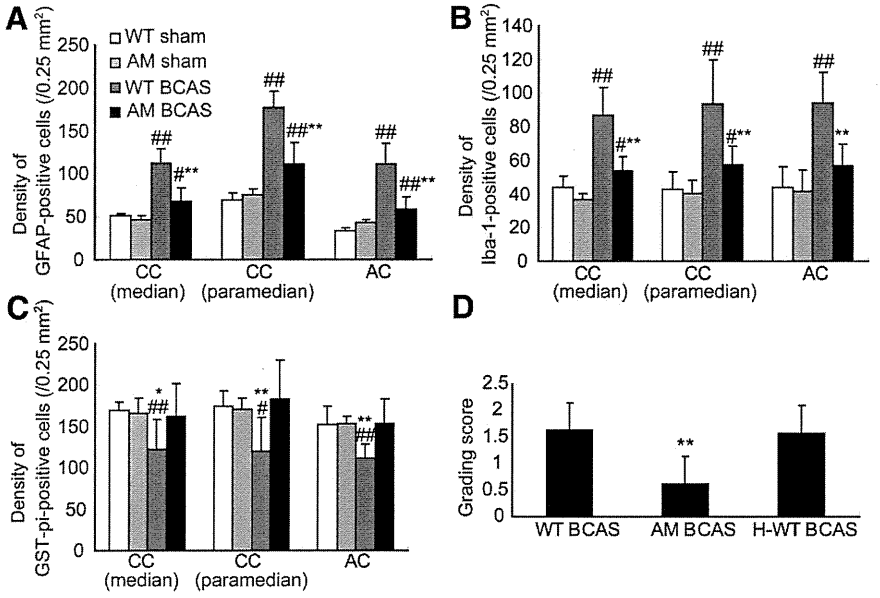

Figure 4. Adrenomedullin (AM) restores white matter integrity after BCAS. Histograms showing the density of cells immunoreactive for GFAP (A), Iba-1 (B), or GST-pi (C) in the medial and paramedial portions of the corpus callosum (CC) and the anterior commissure (AC) of a wild-type (WT) or AM-Tg mouse subjected to sham or BCAS operation on Day 28 (WT sham, n=4; AM sham, n=4; WT BCAS, n=8; AM BCAS, n=8). Error bars indicate SD. *P<0.05, **P<0.01 in AM BCAS vs WT BCAS; #P<0.05, ##P<0.01 vs WT sham. D, Histograms showing grading score of the CC of WT BCAS (n=14), AM BCAS (n=8), and hydralazine-treated WT BCAS (H-WT BCAS; n=7) on Day 28 post-BCAS. Error bars indicate SD. **P<0.01 in AM BCAS vs WT BCAS and H-WT BCAS. BCAS indicates bilateral common carotid artery stenosis; GFAP, glial fibrillary acidic protein; Iba-1, ionized calcium binding adapter molecule 1; GST-pi, glutathione-S-transferase-pi; AM-Tg, mice overexpressing circulating AM.

mice on Day 28 (Figure 4A–C; Supplemental Figure IIA, a–c, e–g, and i–k). In BCAS-operated AM-Tg mice, by contrast, the density of astrocytes and microglia significantly decreased and that of mature oligodendrocytes significantly increased compared with BCAS-operated WT mice (Figure 4A–C; Supplement Figure IIA, d, h, and l). Similarly, BCAS-operated AM-Tg mice on Day 7 showed significantly decreased density of microglia and increased density of mature oligodendrocytes but no difference in the density of astrocytes compared with BCAS-operated WT mice (Supplemental Figure IIB–D).

Klüver–Barrera staining on Day 28 revealed that BCAS-induced WM lesions were predominant in the corpus callosum and the caudoputamen in WT mice (Supplemental Figure IIA, m–o). In AM-Tg mice, such WM lesions became far less severe (Supplemental Figure IIAp). In the hydralazine-treated WT mice, BCAS-induced WM lesions were as severe as those in WT mice, suggesting that such positive effects of AM may be independent of the hypotensive effect of AM (Figure 4D).

Thus, BCAS-induced WM lesions were restored in the AM-Tg mice in parallel with inhibition of glial activation and preservation of mature oligodendrocytes.

Adrenomedullin Prevents Working Memory Deficits After BCAS

To evaluate working memory, we examined a Y maze test and an 8-arm radial maze test. The Y maze test was performed 1 month after the surgery. Alternations of entries in the arms of the Y maze were significantly increased in BCAS-operated AM-Tg mice (64.6%±7.5%) compared with BCAS-operated WT mice (58.2%±8.0%), although alternations of entries were not significantly different between WT and AM-Tg mice after sham operation (Figure 5A). Spontaneous activity was not significantly different among the 4 groups of mice (Figure 5B). In another set of mice, the 8-arm

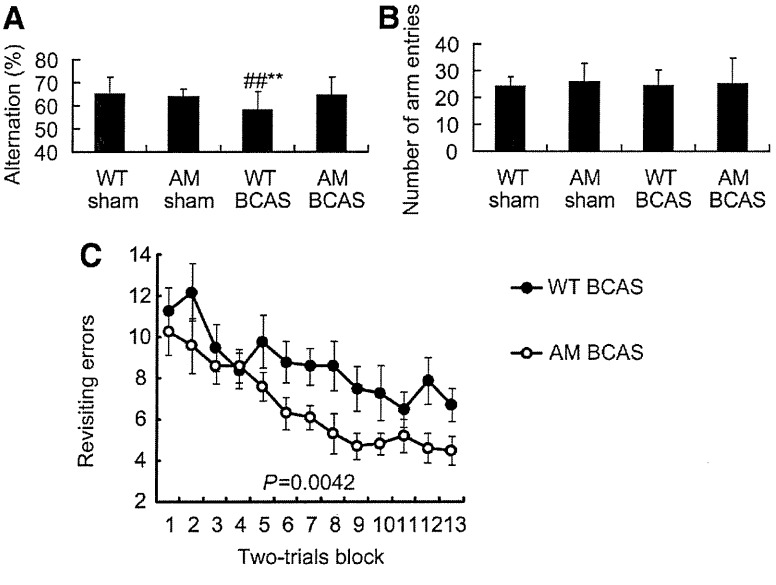

Figure 5. Adrenomedullin (AM) prevents working memory deficits after BCAS. A, Histogram showing spontaneous alternation in the Y maze test of wild-type (WT) or AM-Tg mice at 1 month after sham or BCAS operation (WT sham, n=17; AM sham, n=10; WT BCAS, n=26; AM BCAS, n=17). Error bars indicate SD. **P<0.01 in AM BCAS vs WT BCAS; ##P<0.01 vs WT sham. B, Histogram showing spontaneous activity in the Y maze test. Error bars indicate SD. C, The number of revisiting errors in the 8-arm radial maze test at 1 month after BCAS of WT or AM-Tg mouse (WT BCAS, n=19; AM BCAS, n=17). Values are expressed as means±SEM. BCAS indicates bilateral common carotid artery stenosis; AM-Tg, mice overexpressing circulating AM; AM, adrenomedullin.

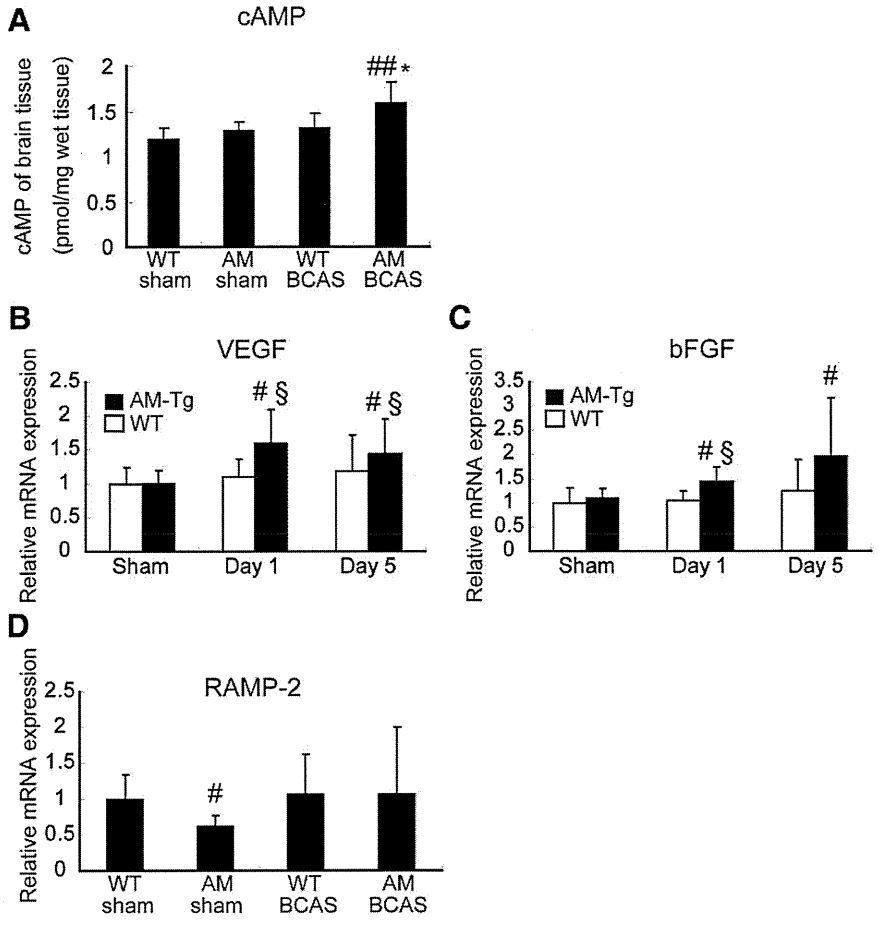

Figure 6. Adrenomedullin (AM) increases brain cAMP, VEGF, and bFGF levels after BCAS. A, Histogram showing brain cAMP levels in wild-type (WT) or AM-Tg mice on Day 5 after sham or BCAS operation (WT sham, n=4; AM sham, n=5; WT BCAS, n=5; AM BCAS, n=5). Error bars indicate SD. *P<0.05 in AM BCAS vs WT BCAS; ##P<0.01 vs WT sham. B–C, Histogram showing mRNA levels of VEGF (B) and bFGF (C) in the brains of WT or AM-Tg mice on Days 1 and 5 (n=5 to 7 each). Error bars indicate SD. #P<0.05 vs WT sham; §P<0.05 in AM sham vs AM BCAS. D, Histograms showing mRNA levels of AM receptor, RAMP2, in the brains of WT or AM-Tg mice subjected to sham or BCAS operation (WT sham, n=7; AM sham, n=5; WT BCAS, n=7; AM BCAS, n=7) on Day 5. The mRNA levels are presented as ratios relative to levels of 18S rRNA. Error bars indicate SD. #P<0.05 vs WT sham. VEGF indicates vascular endothelial growth factor; bFGF, basic fibroblast growth factor; BCAS, bilateral common carotid artery stenosis; AM-Tg, mice overexpressing circulating AM; AM, adrenomedullin; RAMP2, receptor activity-modifying protein-2.

radial maze test was started 1 month after BCAS. BCAS-operated AM-Tg mice showed a significant reduction in the number of revisiting errors compared with BCAS-operated WT mice (Figure 5C). We have found a significant correlation of the averaged number of revisiting errors 1 month after BCAS with CBF on Days 7, 14, and 28, but not with CBF immediately after BCAS, or on Days 1 and 3 (Supplemental Figure III).

Taken together, these results suggest that AM restores working memory deficits induced by BCAS.

Adrenomedullin Increases cAMP Level in the Forebrain After BCAS

The restorative effect of AM described led to the investigation of the underlying mechanisms behind angio-/arteriogenesis and antioxidative activity. The brain level of cAMP, a second messenger known to associate with AM, was therefore measured. A significant increase in the brain level of cAMP was found in AM-Tg mice after BCAS (AM BCAS, 1.6±0.2 pmol/mg wet tissue) compared with WT mice after BCAS (WT BCAS, 1.3±0.2 pmol/mg wet tissue) on Day 5, although the level of cAMP was not different between WT and AM-Tg mice after sham operation (Figure 6A).

These results suggest that chronic ischemic stress induced AM-mediated elevation of cAMP in the brain.

Adrenomedullin Increases mRNA and Protein Levels of Vascular Endothelial Growth Factor and Basic Fibroblast Growth Factor in the Forebrain After BCAS

The reasons behind the apparent AM-initiated signaling pathway-led arteriogenesis and angiogenesis were next examined. Brain levels of vascular growth factors, including vascular endothelial growth factor (VEGF) and basic fibroblast growth factor (bFGF), were therefore measured. The mRNA and protein levels of brain VEGF and bFGF were significantly increased in AM-Tg mice on Days 1 and 5 post-BCAS compared with sham-operated WT mice (Figure 6B–C; Supplemental Figure IV).

Chronic Ischemic Insult Upregulates Brain mRNA Level of Adrenomedullin and Abolishes Receptor Activity-Modifying Protein-2 Suppression Induced by Adrenomedullin

The status of mouse AM, high-affinity AM receptors, calcitonin receptor-like receptors, and Subtypes 2 and 3 of a family of receptor activity-modifying proteins (RAMP2 or 3) were then measured on Day 5. The brain mRNA level of mouse AM was significantly increased (3.1-fold) in BCAS-operated WT mice compared with sham-operated WT mice. In addition, brain RAMP2 mRNA level was significantly lower (0.6-fold) in sham-operated AM-Tg mice compared with sham-operated WT mice. Such downregulation of RAMP2 mRNA